Norsk institutt for luftforskning
Norwegian Institute for Air Research

# Synergistic exploitation of the methane product from Sentinel-5P for applications in the Arctic (STEPS)

Kerstin Stebel, Arve Kylling, Philipp Schneider and Martin Album Ytre-Eide

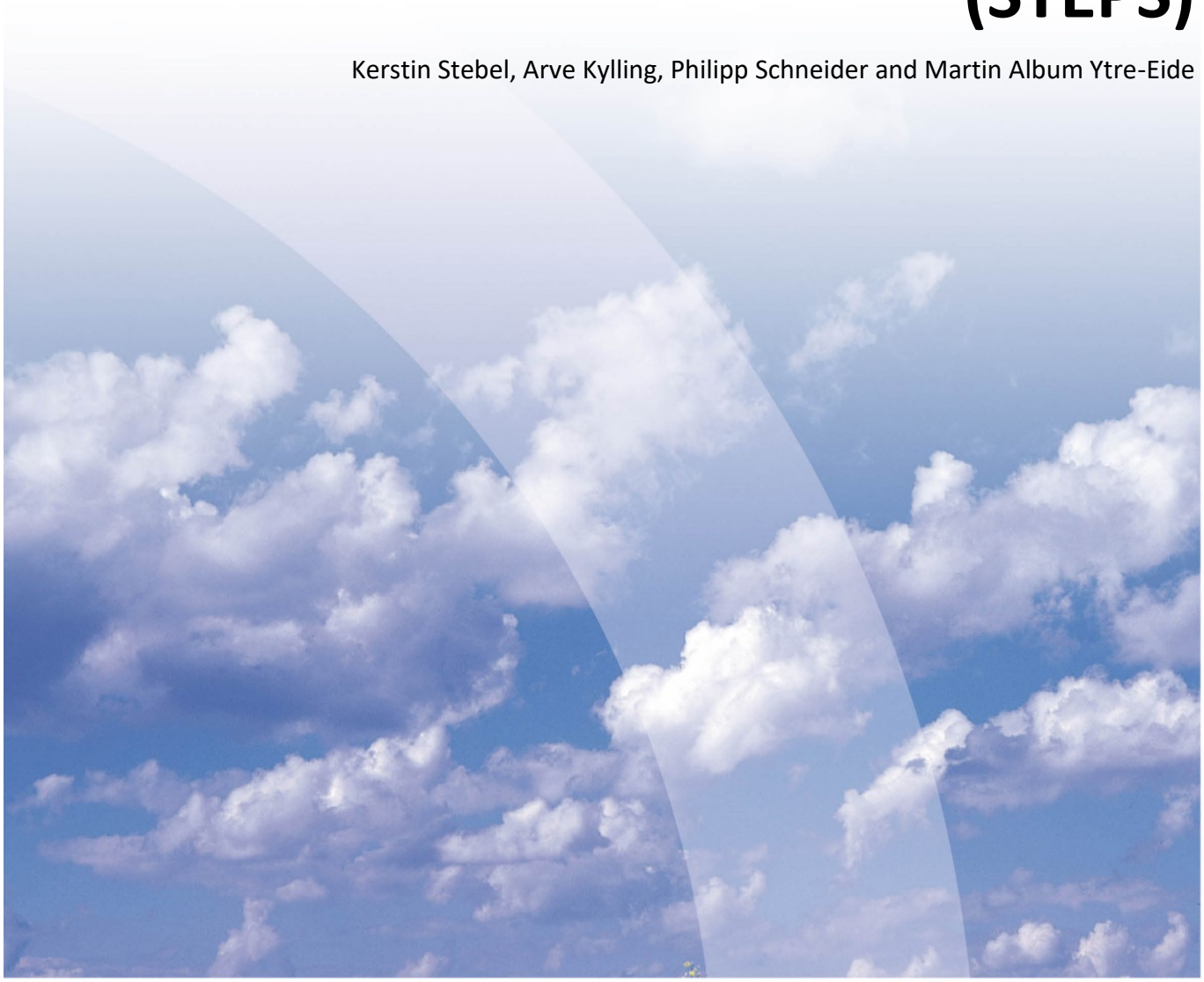

NILU report 14/2022

| **NILU report 14/2022** | ISBN: 978-82-425-3084-4<br>ISSN: 2464-3327 | CLASSIFICATION:<br>A – Unclassified (open report) |
|---|---|---|
| DATE<br>13.05.2022 | SIGNATURE OF RESPONSIBLE PERSON<br>Ole-Anders Braathen (sign.)<br>Deputy director | NUMBER OF PAGES<br>50 |


| TITLE | PROJECT LEADER |
|---|---|
| Synergistic exploitation of the methane product from Sentinel-SP for applications in the Arctic (STEPS) | Kerstin Stebel |
| | NILU PROJECT NO.<br>S-120149 |
| AUTHOR(S)<br>Kerstin Stebel, Arve Kylling, Philipp Schneider and Martin Album Ytre-Eide | QUALITY CONTROLLER<br>Arve Kylling |
| REPORT PREPARED FOR<br>Norsk Romsenter, Postboks 113 Skøyen, 0212 Oslo<br>Att.: Petter Evju Skanke | CONTRACT REF.<br>NIT.14.20.5 |


ABSTRACT

The main goal of this feasibility study was to evaluate the potential of adding value to the Sentinel 5P TROPOMI methane product over Norway and the Arctic through the synergistic use of relevant observations from other Sentinel satellites and machine learning. We assessed the data availability of ESA operational and research-based WFMD $XCH_4$ products over the Northern hemisphere, the Nordic countries and the Arctic/Northern latitudes. ESA's $XCH_4$ data have poor coverage over Norway. Seeing the two datasets as complementary, seems to be the most reasonable approach for utilization them. Furthermore, we investigated potential synergies between satellite products from different platforms. A random forest (RF) machine learning algorithm was implemented. It shows the importance of daytime land surface temperature (LST) as predictor variable for $CH_4$. Our results indicate that the RF-model has a very good capability of filling small gaps in the data.


NORWEGIAN TITLE

Synergistisk utnyttelse av metanproduktet fra Sentinel-SP for anvendelser i Arktis (STEPS)


KEYWORDS

Remote sensing | Methane | Arctic



ABSTRACT (in Norwegian)

Hovedmålet med denne mulighetsstudien var å evaluere potensialet for å tilføre verdi til Sentinel 5P TROPOMI-metanproduktet over Norge og Arktis gjennom synergistisk bruk av relevante observasjoner fra andre Sentinel-satellitter og maskinlæring. Vi vurderte datatilgjengeligheten til ESAs operasjonelle og forskningsbaserte WFMD XCH4-produkter over den nordlige halvkule, de nordiske landene og de arktiske/nordlige breddegrader. ESAs XCH4-data har dårlig dekning over Norge. Å se de to datasettene som komplementære, ser ut til å være den mest fornuftige tilnærmingen for å bruke dem. Videre undersøkte vi potensielle synergier mellom satellittprodukter fra ulike plattformer. En maskinlæringsalgoritme (Random forest, RF) ble implementert. Den viser viktigheten av jordoverflatetemperatur (LST) på dagtid som variabel for $CH_4$. Våre resultater indikerer at RF-modellen har en meget god evne til å fylle små hull i dataene.



| PUBLICATION TYPE: Digital document (pdf) | COVER PICTURE: Source: NILU |
|---|---|





Citation: Stebel, K., Kylling, K., Schneider, P., Ytre-Eide, M.A. (2022). Synergistic exploitation of the methane product from Sentinel-SP for applications in the Arctic – STEPS (NILU report 14/2022). Kjeller: NILU.

NILU's ISO Certifications: NS-EN ISO 9001 and NS-EN ISO 14001. NILU's Accreditation: NS-EN ISO/IEC 17025.

# Table of Contents

# Summary

***The main goal of this feasibility study was to evaluate the potential of adding value to the Sentinel-5P TROPOMI methane product over Norway and the Arctic through the synergistic use of relevant observations from other Sentinel satellites and machine learning.***

We first assessed the data availability of operational TROPOMI and the research-based, no-operational WFMD $XCH_4$ products over the Northern hemisphere, the Nordic countries and the Arctic/Northern latitudes. Effects of quality control and bias correction of the operational data were analysed. Quality flag and the bias correction corrects the $XCH_4$ underestimation for low albedo values, and reduces the overestimation for high albedo values over desert areas, and make the operational data more comparable to the most recent WFMD $XCH_4$ product. For the Nordic countries and the boreal forest region in Russia, the operational data are about 10-20 ppb lower than the WFMD $XCH_4$ values. A main caveat of the operational ESA $XCH_4$ data is its poor coverage over Norway, and that there are no data available over the ocean. Due to the low data coverage, the initially planned additional filtering to generate improved seasonal $CH_4$-maps did not seem useful to be performed within the STEPS projects.

We further investigated potential synergies between satellite products from different platforms to add value to the operational TROPOMI $CH_4$ data products. A random forest (RF) machine learning (ML) algorithm was implemented. As predictor variables, we used NDVI, land cover, elevation, daytime and night-time land surface temperatures (LST), black- and white sky albedo and surface soil moisture data. The results indicate that by the far the most important variable for predicting $XCH_4$ in this case study is the daytime LST, followed by night-time LST and white-sky albedo. NDVI, which has been exclusively used for example by Zhang et al (2012) for gap-filling and downscaling $XCH_4$, ranks only in fourth position in our case study. Our results indicate that the RF-model has a very good capability of filling small gaps in the data with a prediction accuracy on the same order of magnitude as the difference between the operational and WFMD products. It should be noted that ML-algorithms can typically only predict well for conditions that they have been previously trained for. This has an implication on filling gaps over mountainous areas in Norway since the operational TROPOMI $XCH_4$ product is typically not retrieved over mountain areas.

The WFMD-data show better coverage, including data over the ocean, but these data are only available until the end of 2020, and are not provided in near-real-time. Reprocessing of the operational data was announced for 2022, and it is expected that the upcoming version will have better data coverage. Nevertheless, it remains to be seen, which improvements will be made during the re-processing and how this will affect availability and quality of the data over the Norwegian territory, Northern latitudes and the Arctic. Meanwhile, seeing these two versions as complementary – as mini-ensemble, seem to be the most reasonable approach for utilization of the Sentinel-5P $XCH_4$ data.

# SynergisTic Exploitation of the methane Product from Sentinel-SP for applications in the Arctic (STEPS)

## 1 Introduction

The main goal of this feasibility study was to evaluate the potential of adding value to the Sentinel-5P TROPOspheric Monitoring Instrument (TROPOMI) methane ($CH_4$) product over Norway and the Arctic through synergistic use of relevant observations from other Sentinel satellites and machine learning. In more detail, the STEPS project aimed at:

- an assessment of the spatial and temporal patterns in data availability of the TROPOMI $CH_4$ product over regions of Norway and the Arctic, including an evaluation of possible reasons,
- the generation of improved seasonal $CH_4$ maps by filtering questionable retrievals using information from related Sentinel data,
- an investigation of products from other Sentinels to detect and quantify potential correlations in spatiotemporal patterns with the TROPOMI $CH_4$ product, and
- to assess further potential of the synergistic exploitation of the data by implementation of a machine learning algorithm.

Methane emissions to the atmosphere are both anthropogenic (approximately 60%) and biogenic (approximately 40%, Saunois et al., 2020). It is the second most important anthropogenic greenhouse gas after carbon dioxide ($CO_2$). Therefore, it plays an essential role in NILU's scientific and operational monitoring activities. On behalf of the Norwegian Environment Agency, NILU performs and reports measurements of 40 greenhouse gases, including $CO_2$ and $CH_4$, at Zeppelin (474 m a.s.l., 78°54'29" N, 11°52'53" E) and Birkenes (190 m a.s.l, 58°23'N, 8°15'E) (Myhre et al., 2021; Platt et al., 2018; Nisbet et al., 2019). These observations contribute to the research infrastructure ICOS (Integrated Carbon Observation System, Heiskanen et al., 2022). Figure 1 shows the long-term $CH_4$ observations made at the two sites. A record increase was observed to reach 1968.7 ppb at Zeppelin and 1975.2 ppb at Birkenes. At Zeppelin there are now 20 years of data, showing a trend of +6.4 ppb or 0.3% per year. For Birkenes, the time series is shorter and the trend analysis, +8.4 ppb or 0.4% per year for the period 2009-2020, is less accurate. Growth rates for 2019-2020 were: + 15.7 ppb at Zeppelin and + 14 ppb at Birkenes.

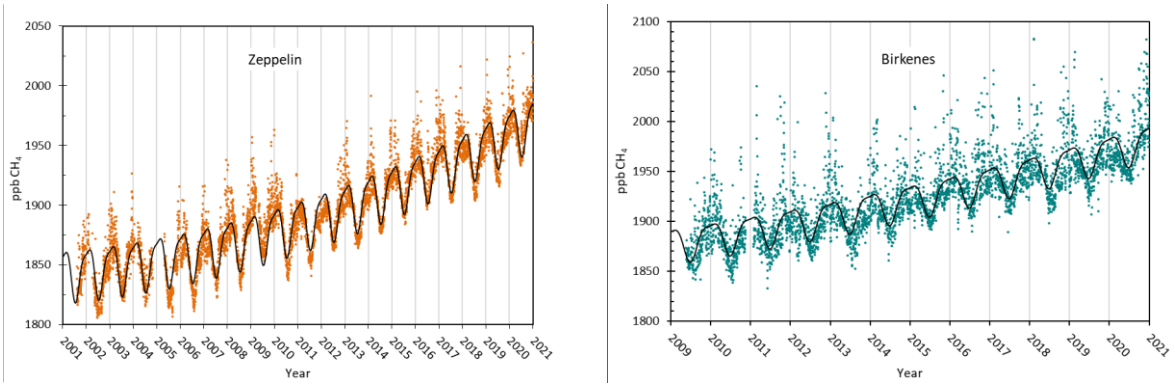


Figure 1: *The left panel shows observations of daily averaged methane mixing ratio for the period 2001-2020 at the Zeppelin Observatory. The black solid line is empirical fitted methane mixing ratio. The right panel shows the daily mean observations for Birkenes (green dots). [equal to Figure 9 in Myhre et al., (2021)]*

So far, methane distributions and flux estimates in Europe and Northern latitudes, were constrained with surface observations only (Thompson et al., 2017, Groot Zwaaftink et al., 2018). The recently started NFR-funded ReGAME project (Reliable global methane emissions estimates in a changing world) project (2021-2025), which is coordinated by NILU, includes a task of updating the inversion models to include TROPOMI $CH_4$ data fields and of assessing the effect this has on the resulting methane fluxes.

To support NILU's scientific and operational monitoring activities, the STEPS project was initiated. The work was inspired by the early study of Zhang et al. (2012), who used ordinary kriging and ordinary cokriging to interpolate and downscale atmospheric $CH_4$ column concentrations from the SCIAMACHY/ENVISAT instrument using the normalized difference vegetation index (NDVI) from MODIS from 50 km to 5 km spatial resolution. As TROPOMI measures methane total column-averaged dry-air mole fraction ($XCH_4$) at a resolution of 7.0 km to 5.5 km (since 6 August 2019), we find not much need for additional downscaling, but the multi-sensor information can give us a much better understanding of the $CH_4$ abundance, emission sources and potentially data quality. A pre-deposit for this is the TROPOMI $XCH_4$ data quantity and quality, which was studied in more detail in Task 1.

# 2 Task 1: TROPOMI $CH_4$ data availability in Norway and the Arctic

The goal of Task 1 was to lay the foundation for the STEPS project, by carrying out a literature review and providing an assessment of the spatiotemporal availability of the TROPOMI operational $CH_4$ data product for Norway and the Arctic. For this, the operational ESA TROPOMI/S5P Methane Level-2 Swath 7.0 km x 7.0 km (7.0 km to 5.5 km along track starting from 6 August 2019, orbit 9388) offline data product was downloaded from the Copernicus S5P Open Access Hub (https://scihub.copernicus.eu/). Data are from processor versions 01.02.02 – 02.03.01. For further analysis, the Level-2 data were re-gridded to daily data files with 0.1° x 0.1° resolution using the HARP tools (https://stcorp.github.io /harp/doc/html/index.html). Software for reading and plotting of various $CH_4$ data (various products, temporal, and spatial selections) was developed.

Satellite $CH_4$ data are generally given as methane total column-averaged dry-air mole fraction ($XCH_4$), which is the total atmospheric column between the surface and the top of the atmosphere normalized to the corresponding dry air column. The operational ESA algorithm to generate $XCH_4$, based on TROPOMI measurements of sunlight backscattered by Earth's surface and atmosphere in the near-infrared (NIR) and shortwave-infrared (SWIR) spectral bands, was developed by SRON and is described in Hu et al. (2016), Landgraf et al. (2019) and Hasenkamp et al. (2021). Hu et al. (2018) showed the first global methane observations from TROPOMI. A revised and improved operational product, showing less biases, is described by Lorente et al. (2021). A major caveat with the operational $XCH_4$ product is its reported dependency on surface albedo (Schneising et al., 2019; Lorente et al., 2021). An albedo climatology is used, which can deviate from the real albedo.

Besides $XCH_4$ ("methane_mixing_ratio"), the files also contain data corrected for the XCH4 dependence on surface albedo ("methane_mixing_ratio_bias_corrected"). More information on the a-posteriori correction can be found in the Algorithm Theoretical Basis Document (ATBD) (Hasenkamp et al., 2021), and in Lorente et al. (2021). In the initial operational version this correction was based on the comparison of TROPOMI $XCH_4$ with GOSAT retrievals. After two years a new bias correction based only on TROPOMI data was implemented. Small enough areas, assuming constant $XCH_4$, but large albedo variations around the globe are selected. Subsequently a $XCH_4$ reference value for a surface albedo around 0.2 is estimated, and the ratio of the retrieved $XCH_4$ to the reference value is obtained to estimate the albedo dependence.

It is recommended to use TROPOMI $CH_4$ bias corrected data associated with a quality assurance value qa_value > 0.5 (Landgraf et al., 2021). Landgraf et al. (2021) define the criteria for qa_value = 0.4 as following (note, qa_value = 0.5 is not given):

- Not confidentially clear sky (VIIRS, non-scattering retrieval as back-up)
- Solar zenith angle (SZA) > 70°
- Surface albedo (SWIR) < 0.02
- Aerosol optical thickness AOT (NIR) > 0.3
- $CH_4$ noise related error > 10
- Chi squared of fit $\chi^2$ > 100
- Terrain roughness > 80

To further cite Landgraf et al. (2021) "Filtering on qa_value > 0.5 does not remove all pixels considered bad. Some pixels with too low methane concentrations are still present." As shown below, also some areas with too high methane concentrations are not filtered out properly yet.

The data quality criteria severely affect the data coverage, particularly over Norway (where the terrain roughness criteria leads to removal of data in the mountain regions), thus additional filtering, which was initially planned as a measure to improve data quality, did not seem suitable within the STEPS project.

To better understand the operational $XCH_4$ data quantity and quality, it was found important to compare the operational ESA data to an alternative scientific methane retrieval. This retrieval is described in Schneising et al (2019) who used Weighting Function Modified DOAS (WFMD) to simultaneously retrieve column-averaged dry air mole fractions of atmospheric $CH_4$ and CO from the shortwave-infrared (SWIR) nadir spectra of TROPOMI (Product ID: CH4_S5P_WFMD). The data were produced at the Institute of Environmental Physics at the University of Bremen in the framework of the ESA GHG-CCI+ project. The data set, covering November 2017 to December 2020 was download from http://www.iup.uni-bremen.de/carbon_ghg/products/tropomi_wfmd. We used data from the baseline version v1.2 and the recent released product version v1.5. The changes made between the two versions are described in the ATBD (see Schneising, 2021). They encompass processing- as well as post-processing steps, such as, e.g., the resolution of the surface elevation and additional surface roughness information, an extension of the training data set for the random forest classifier, additional features, and a quality filter.

In the following we show a number of exemplary comparisons of the operational ESA and the WFMD $XCH_4$ datasets. As a reference month we use June 2020, where data occurrence is high compared to the winter months (when no or little sunlight is available due to low sun angle and clouds are frequent). See also the feasibility study, which was prepared in 2021 for the Norwegian Environment Agency (Kylling et al., 2021). Monthly averaged, bias corrected, quality flagged $XCH_4$ data from the operational, as well from the WFMD retrieval version 1.5 for the entire time between 2018 and 2020 for the Northern latitudes and the Arctic are shown in Appendix A and Appendix B, respectively.

## 2.1 TROPOMI $XCH_4$ data for the Northern hemisphere

Figure 2 shows examples of monthly averaged HARP re-gridded operational $XCH_4$ for the northern hemisphere for June 2020. We show data without quality flag applied, data with recommended quality flag (qa_value > 0.5), and quality flagged data, which have been bias corrected. For the WFMD retrieval, methane concentrations are shown in Figure 5, both for version 1.2 and version 1.5.

The operational ESA product has no data over the ocean, these are excluded due to low signal over the sea. A strong gradient in $XCH_4$ can be seen from the equator northwards, in particular between the boreal forest region in latitudes above 50°N and the African Saharan region (Figure 2, upper panel). This may be caused by albedo assumptions made for the operational retrieval. This gradient is less pronounced once the quality filter is applied (Figure 2, middle panel). As described by Hasenkamp et al. (2021), the bias correction corrects the $XCH_4$ overestimation for high albedo values over desert areas like Sahara, and the $XCH_4$ underestimation for low albedo values (e.g. over Northern latitudes). Lorente et al. (2021) found a low bias of 39.4 ppb for the non-bias corrected data, when compared to Total Carbon Column Observing Network (TCCON) measurements. According to Hasenkamp et al. (2021), the correction is in the range of 2 %. The effect can be clearly seen when comparing the middle and lower panels in Figure 2.

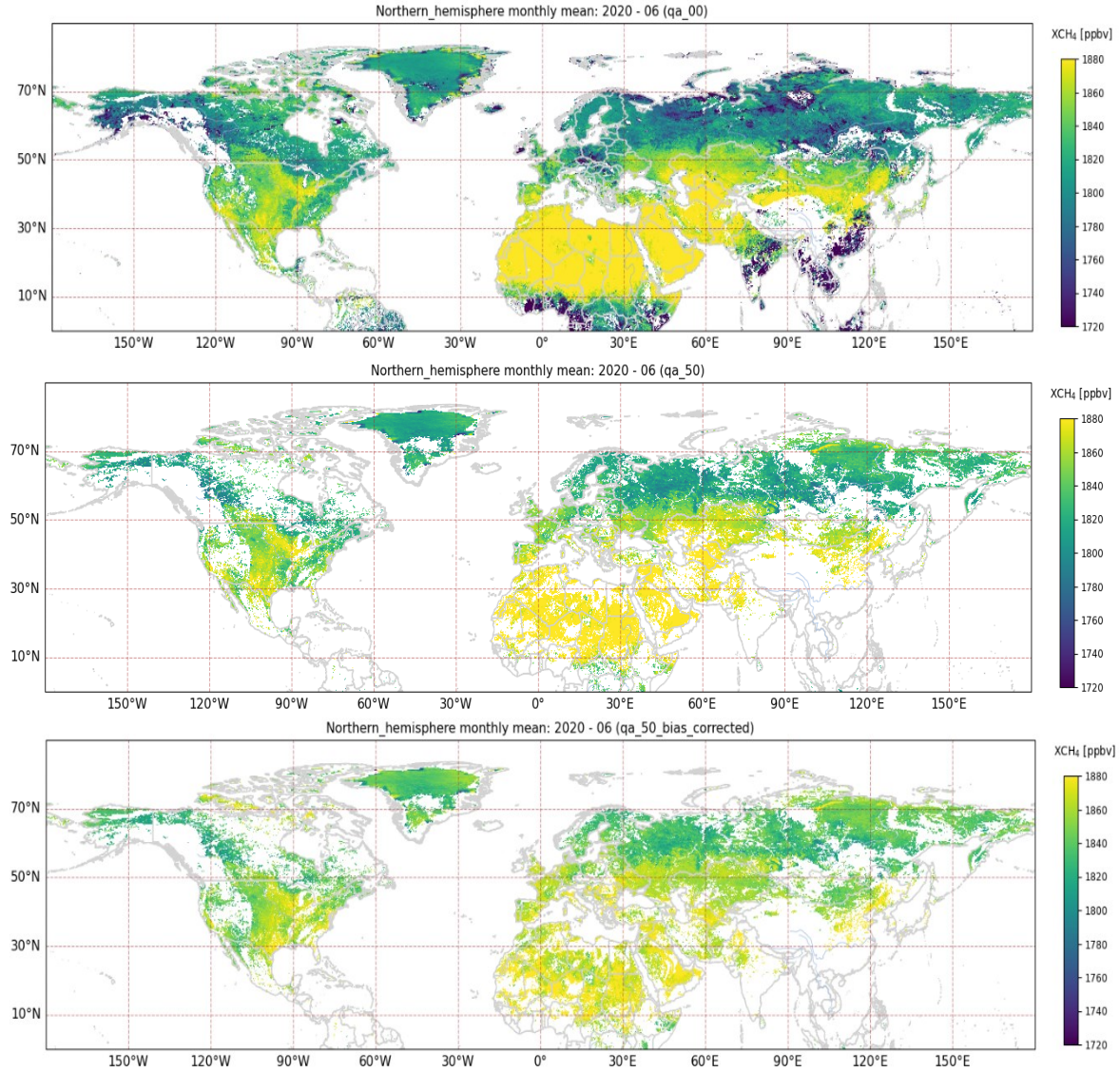


*Figure 2: Monthly averaged ESA operational $XCH_4$ data. Upper panel: Methane mixing ratio without quality-filter; middle panel: $XCH_4$ with quality flag set to > 0.5, lower panel: bias corrected methane mixing ratio with quality flag > 0.5. All plots show mean values for June 2020.*

To illustrate the differences between the non-quality controlled, quality controlled, and additionally bias corrected data, in Figure 3 differences between the non-quality controlled and the quality controlled data (upper panel), as well as the quality controlled bias corrected and the quality controlled non-bias corrected data (lower panel) are shown. The effect of the selections criteria is clearly seen: approximately ± 10 ppb - 15 ppb changes in the monthly averaged $XCH_4$ data due to quality flagging, and circa ± 20 - 30 ppb change due to bias correction. Regionally, both corrections go in the same directions: quality flag and the bias correction corrects the $XCH_4$ underestimation for low albedo values, and reduces the overestimation for high albedo values over desert areas.

In Figure 4, the data coverage for $XCH_4$ is illustrated for the non-quality (upper panel) and quality flagged data (lower panel). It shows the reduction of the data coverage due to quality flagging, in particular in high-albedo regions, e.g., the Sahara, middle-East, but also in middle/western US, Siberia, and parts of Greenland. See Chapter 2.2 and Chapter2.3 for more details in the Nordic countries and the Arctic.

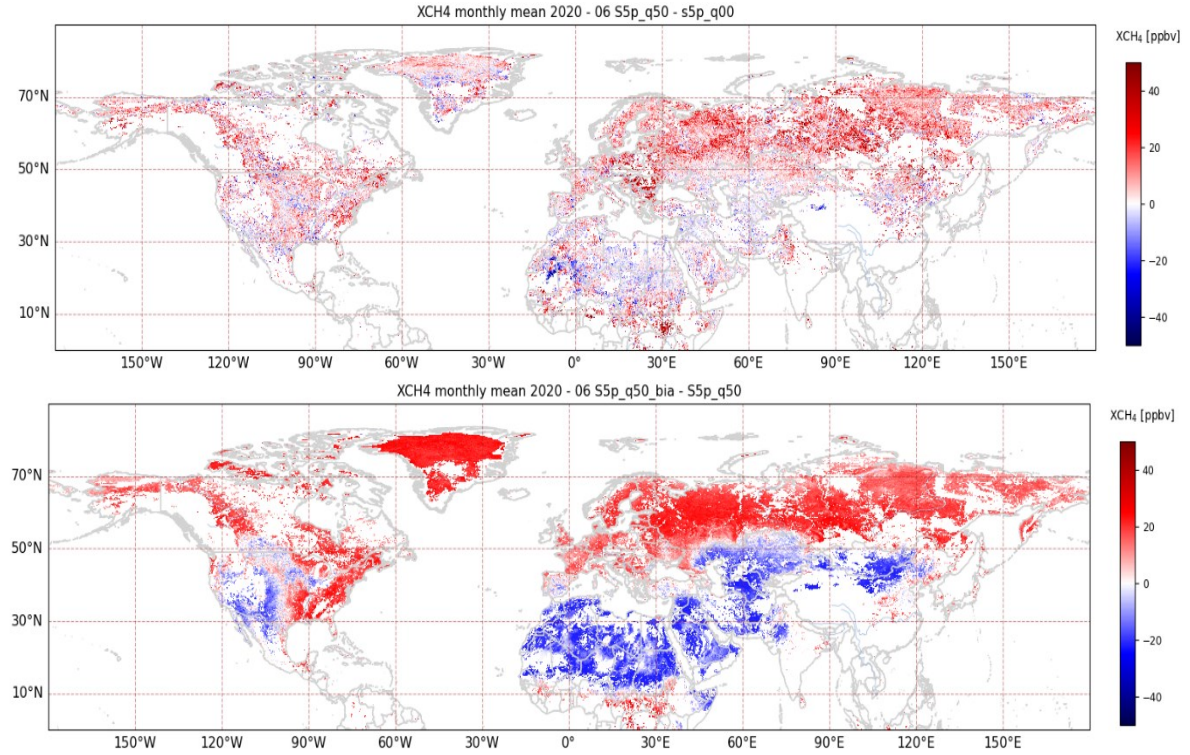


*Figure 3: Differences between monthly averaged operational $XCH_4$ data, illustrated for the dataset for June 2020. Upper panel: differences between data with (qa_value > 0.5) and without quality control flag applied; lower panel: differences between bias corrected and non-bias corrected data (both with qa_value > 0.5).*

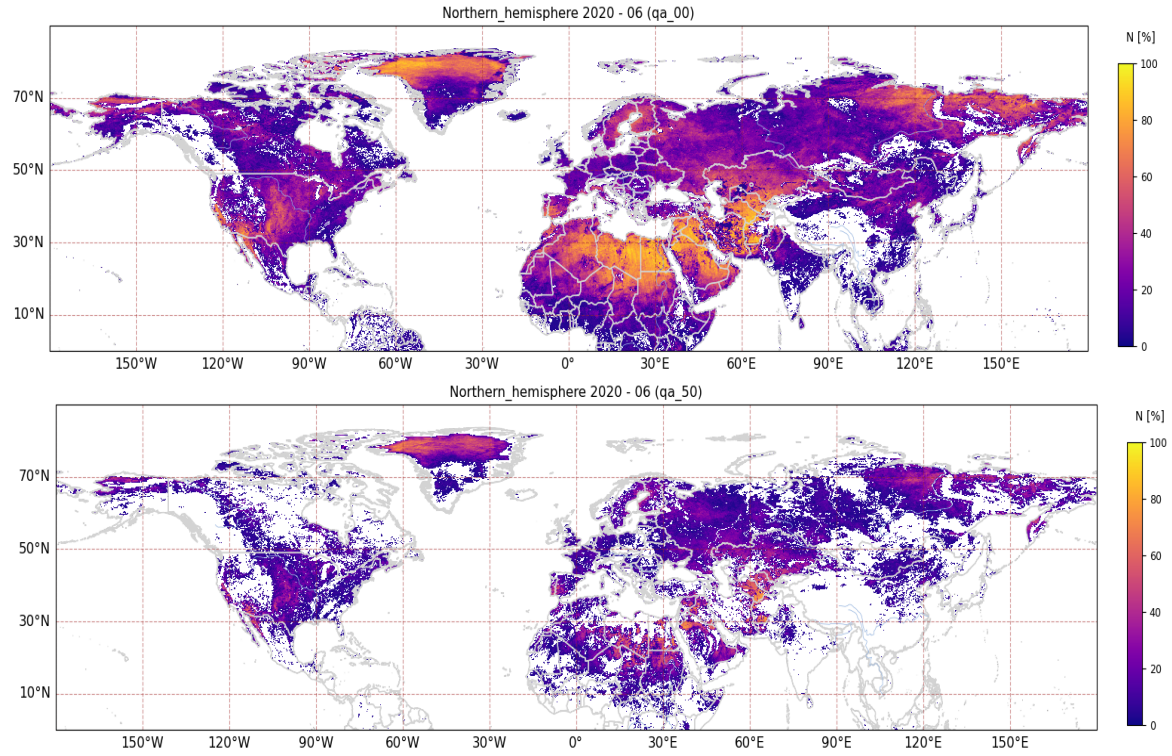


*Figure 4: Data coverage in June 2020. Upper panel: Percentage of days with $XCH_4$ data pixels for non-quality controlled values; lower panel: analogue for quality controlled (qa_value > 0.5) $XCH_4$ data.*

Analogue to the above analysis, in Figure 5 we show the two version, 1.2 and 1.5, of the monthly mean WFMD $XCH_4$ retrieval for June 2020. Most striking, in comparison to the operational product, is that also some data over the ocean and mountain areas are provided. The amount of satellite $XCH_4$ pixel provided increased from version 1.2 to version 1.5. The differences between the two versions is shown in Figure 6. The monthly mean for June 2020 increases in northern latitude, Arctic, as well as in the Sahara, while in the US, Atlantic ocean 20°N - 40°N and central Asia shows lower values in version 1.5 compared to version 1.2. Figure 7 shows the data coverage for the two version for June 2020. Highest values are seen in the US, particular at the west-coast, middle East and south-west Asia. This is a combination of valid retrieval, particularly in high-albedo regions, and clear sky conditions. Data coverage in these areas stays high in version 1.5, and additional regions, which did not have coverage in version 1.2, were filled with data in the most recent data version.

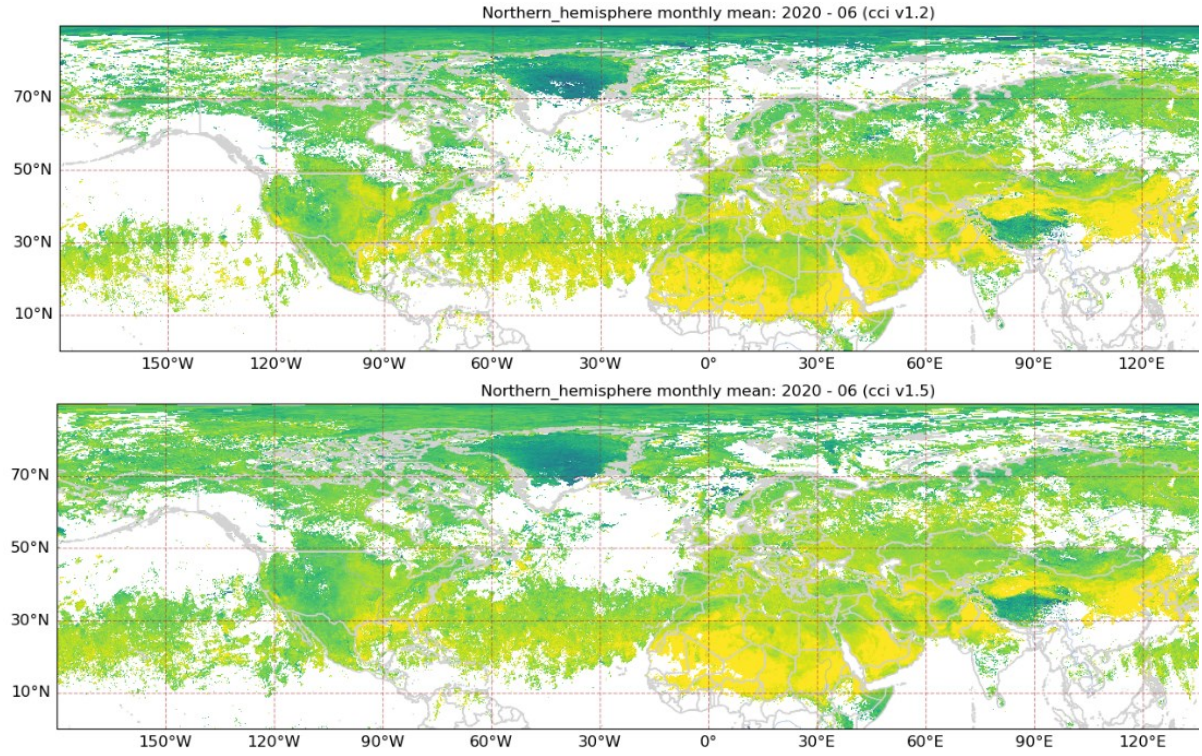


*Figure 5: Monthly mean WFMD $XCH_4$ data for June 2020. Upper panel: $XCH_4$ data version 1.2; lower panel: $XCH_4$ data version 1.5.*

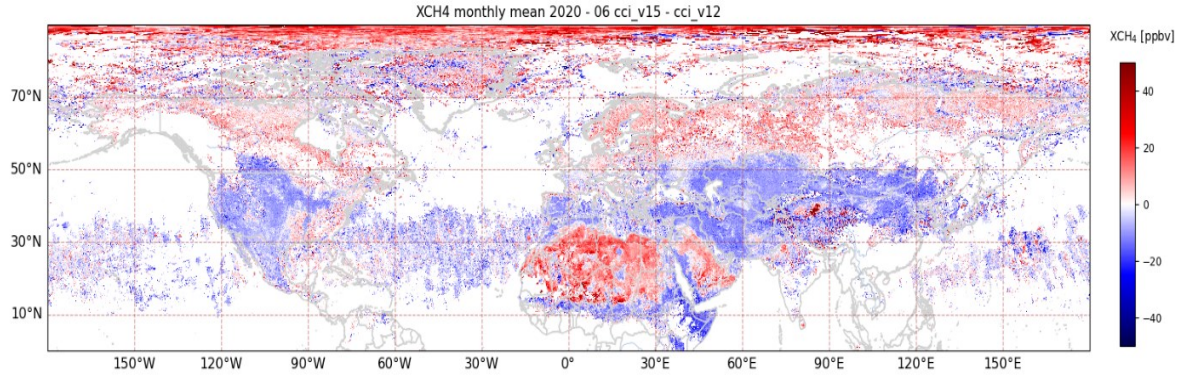


*Figure 6: Difference between WFMD $XCH_4$ data for June 2020 version 1.5 and version 1.2*

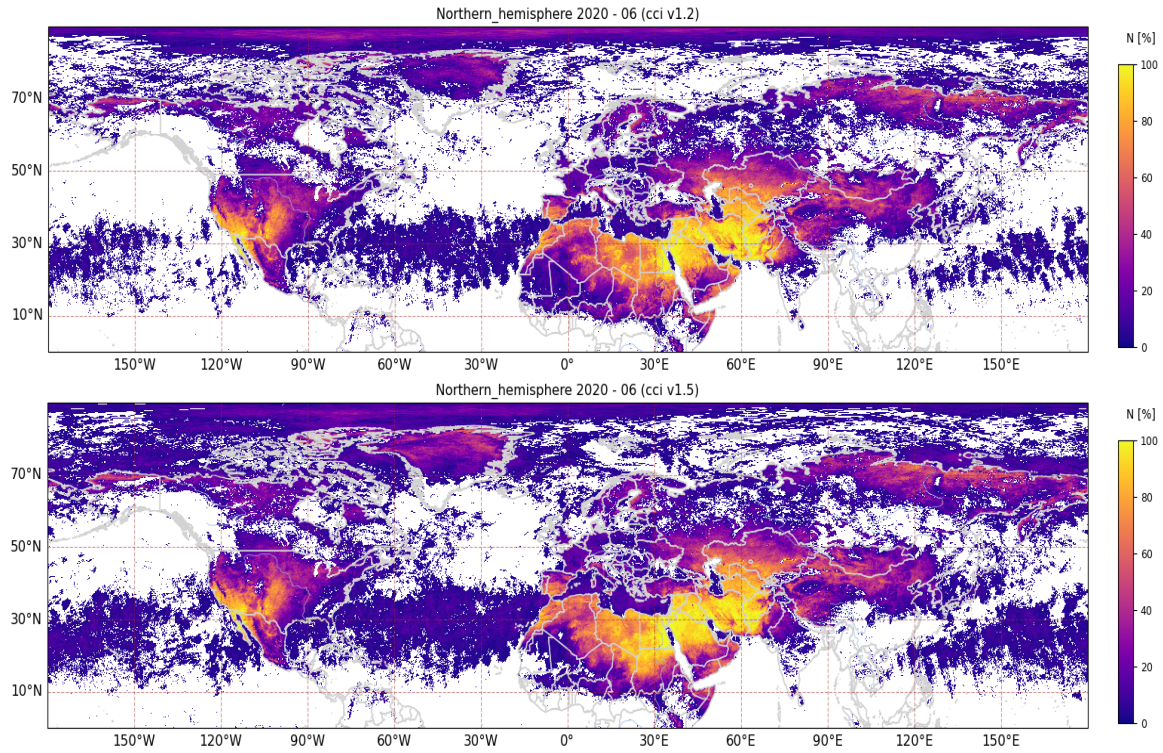


*Figure 7: Data coverage in June 2020. Upper panel: Percentage of days with WFMD $XCH_4$ data pixels for version 1.2; lower panel: analogue for version 1.5*

## 2.2 TROPOMI $XCH_4$ data for the Nordic countries

We are now zooming in to see the differences of the various data versions with respect to the Nordic countries in more detail. Figure 8 shows the monthly mean $XCH_4$ values for the ESA operational retrieval (upper panels) as well as the WFMD $XCH_4$ retrieval (lower panels). Again, the same sub-categories are shown: the non-quality controlled data, the data applied a quality-flag of 0.5, and the quality-flagged and bias corrected data, as well as the two versions of the ESA-CCI+ data. As data with low values seem to be filtered out by applying the quality filter, the monthly mean increase as an effect of the quality restriction, and an additional increase is caused by the bias-correction. These two operations make the operational $XCH_4$ data more comparable to the WFMD $XCH_4$ data.

The operational ESA $XCH_4$ product has poor coverage over Norway. This is because data collected in mountain areas or areas with large height differences within a pixel are filtered out in the analysis chain. This is a main caveat with respect to usability of the ESA operational data for Norway. The WFMD data show better coverage, also over the ocean, but these data are only available until the end of 2020, and are not provided in near-real-time.

Analogue to Figure 3 and Figure 6, in Figure 9 the differences between the non-quality controlled and the quality controlled data (left panel), the quality controlled bias corrected and the quality controlled non-bias corrected data (middle panel), and the difference between the two ESA CCI+ versions (right panel) are shown. The slight increase of the monthly mean $XCH_4$ due to filtering out lower values during quality control, and the stronger increase due to bias correction is evident. Monthly mean WFMD $XCH_4$ version 1.5 data are somewhat higher over land compared to the $XCH_4$ version 1.2 data. Over the ocean positive and negative adjustments are visible.

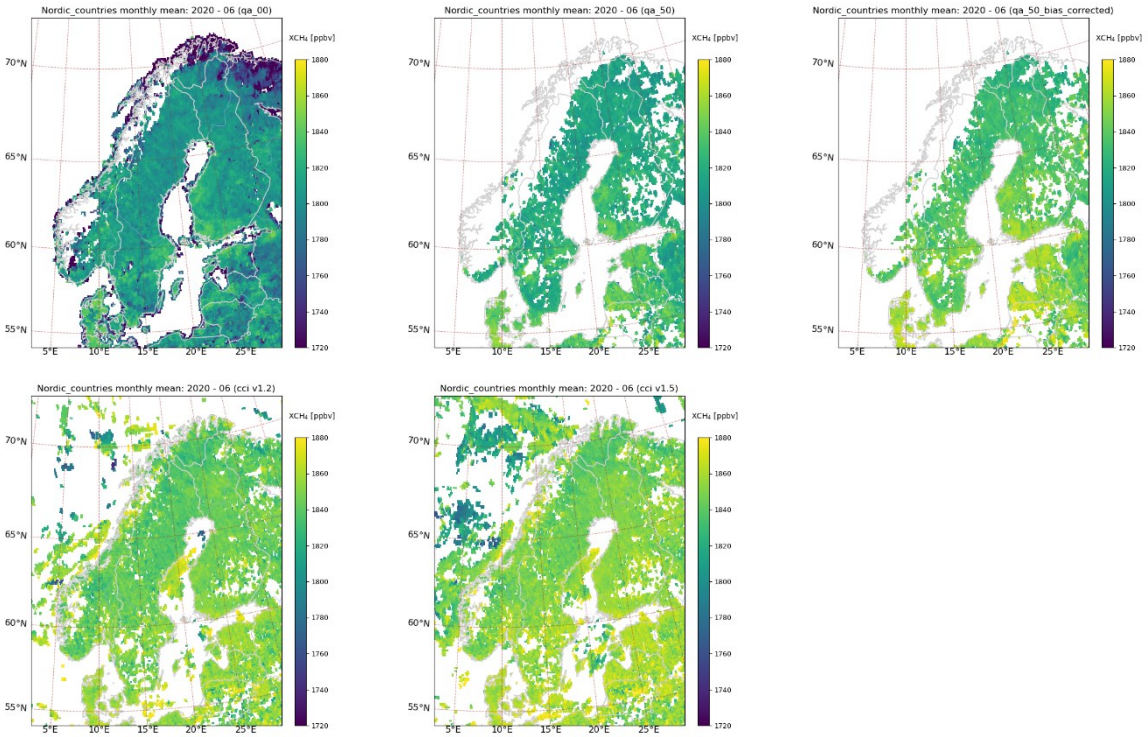


*Figure 8: Examples of monthly averaged operational $XCH_4$ data for the Nordic countries. Upper panels: Operational ESA methane mixing ratio for June 2020. Upper left: without quality-filter; upper middle panel: with quality flag set to > 0.5, upper right panel: bias corrected quality controlled data. Lower panel: WFMD $XCH_4$ data for the same months. Lower left panel: data version 1.2; lower right panel: data version 1.5.*

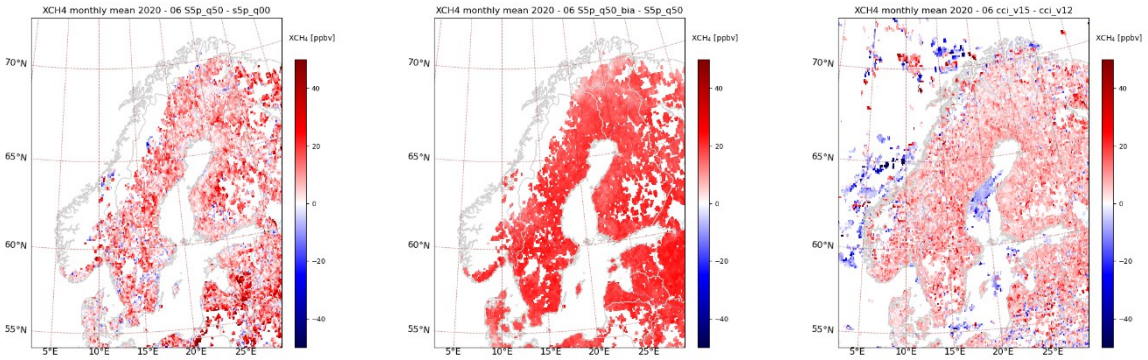


*Figure 9: Differences between monthly averaged ESA operational and WFMD $XCH_4$ data, illustrated for the dataset for June 2020. Left panel: differences between ESA data with (qa_value > 0.5) and without quality control; middle panel: difference between bias corrected and non-bias corrected ESA $XCH_4$ data (both with qa_value > 0.5).Right panel: differences between WFMD $XCH_4$ data version 1.5 and version 1.2*

With respect to data coverage, below we show results from an initial study for Norway. The coverage of the non-quality filtered operational data was analyzed for the counties in Norway (as defined in 2018). Results are show in Figure 10 and are summarized in Table 1. Table 1 shows the number of days per year when the coverage (C) for each county is larger than 10, 25, 50 and 75%. The coverage is poor for counties with large mountain ranges and fiords, that is "Sogn og Fjordane", "Møre og Romsdal", "Hordaland" and "Nordland". Furthermore, the strong North-South gradient is evident, with reasonably good data coverage only in the southernmost counties "Akershus", "Østfold", "Oslo" and "Vestfold". Due to the yearly cycle of the solar zenith angle, there are specific times of the year where there are no data available above specific latitudes (e.g., latitudes above 50°- 60° in the Northern hemisphere winter.

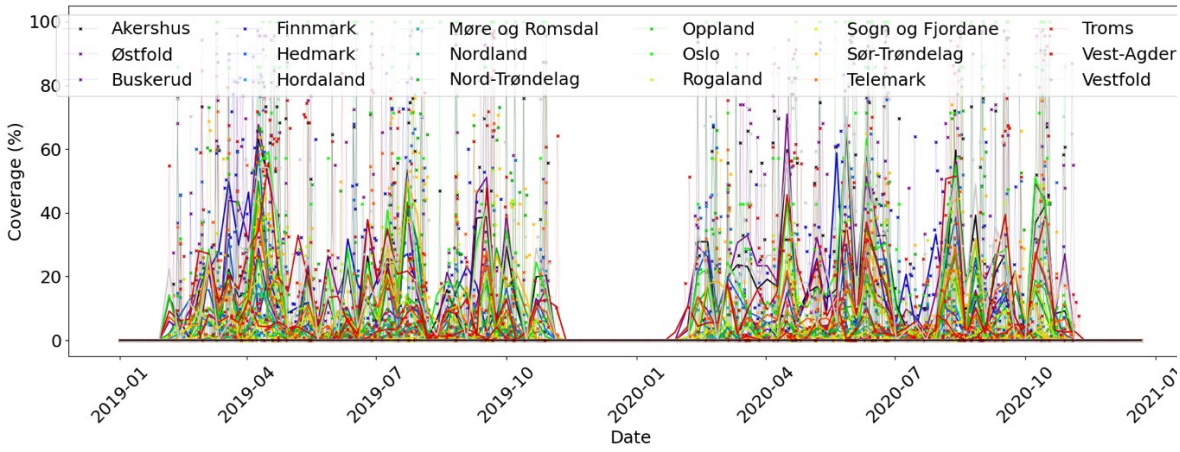


*Figure 10: Data coverage in the various counties of Norway (as defined in 2018).*

*Table 1: Number of days per year when the data coverage (C) for each county is larger than 10, 25, 50 and 75%.*

| ***County*** | ***C > 10%*** | ***C > 25%*** | ***C > 50%*** | ***C > 75%*** |
|---|---|---|---|---|
| Akershus | 91.0 | 71.0 | 53.0 | 29.0 |
| Østfold | 102.5 | 81.5 | 58.5 | 39.5 |
| Buskerud | 72.0 | 38.0 | 6.5 | 0.5 |
| Finnmark | 82.0 | 50.5 | 18.5 | 4.5 |
| Hedmark | 79.5 | 45.5 | 19.0 | 5.0 |
| Hordaland | 37.0 | 6.0 | 0 | 0 |
| Møre og Romsdal | 3.5 | 0 | 0 | 0 |
| Nordland | 9.0 | 0 | 0 | 0 |
| Nord-Trøndelag | 59.0 | 39.5 | 17.5 | 3.0 |
| Oppland | 55.0 | 22.0 | 0.5 | 0 |
| Oslo | 76.0 | 66.0 | 50.0 | 36.0 |
| Rogaland | 62.5 | 35.5 | 0.5 | 0 |
| Sogn og Fjordane | 0 | 0 | 0 | 0 |
| Sør-Trøndelag | 72.5 | 41.5 | 17.5 | 2.5 |
| Telemark | 81.5 | 40.5 | 11.0 | 0.5 |
| Troms | 26.5 | 3.5 | 0 | 0 |
| Vest-Agder | 95.5 | 68.5 | 42.5 | 15.5 |
| Vestfold | 91.0 | 78.5 | 57.0 | 38.5 |

Furthermore, the coverage of the various version is visualized in Figure 11. As pointed out earlier, data coverage is a combination of retrieval specifics and cloud cover. The upper panel shows the non-quality controlled and quality controlled operational data, the lower panel the two version of the WFMD $XCH_4$ data. Effect of the application of the quality flag can be seen, with loss of most data over large areas of Norway, and the reduction from around 40-60% to 10-20% coverage over Sweden. The coverage of the WFMD data is in many regions somewhat higher (around 20-30%), and in particular the availability of data over the Norwegian and the Baltic seas are striking.

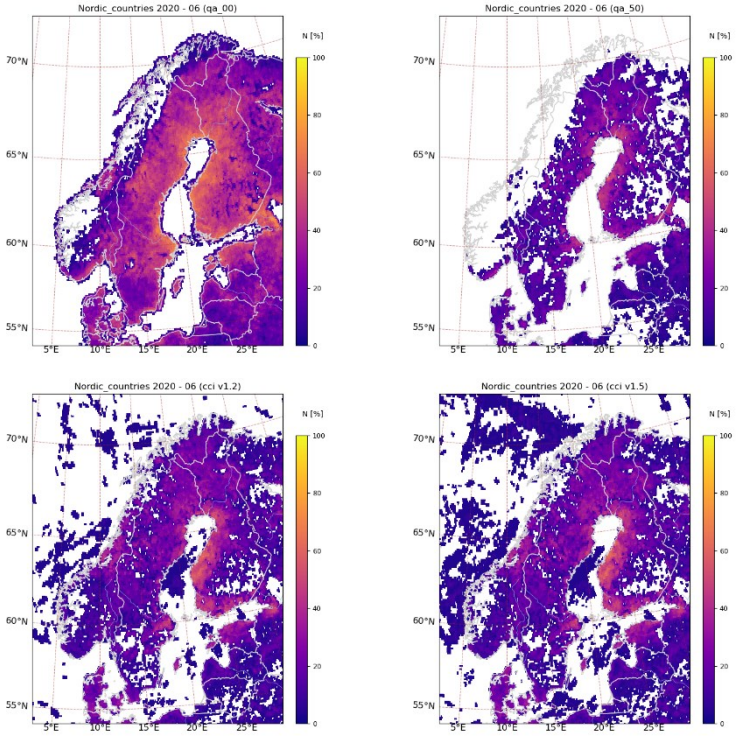


*Figure 11: Data coverage in June 2020. Upper left panel: Percentage of days with $XCH_4$ data pixels for non-quality controlled values; upper right panel: analogue for quality controlled (qa_value > 0.5) $XCH_4$ data. Lower left panel: Percentage of days with WFMD $XCH_4$ data pixels for version 1.2; Lower right panel: analogue version 1.5.*

## 2.3 TROPOMI $XCH_4$ data in the Arctic and Northern latitudes

Analogue to the Figures shown above for the Nordic countries, Figure 12, Figure 13, and Figure 14 show the $XCH_4$ products (various versions), the difference between them, and the data coverage. In addition to the observations described above, it can be seen that the bias-corrected, quality-controlled operational $XCH_4$ observations are somewhat lower than the WFMD $XCH_4$ in Scandinavia and Northern Russia, while for certain areas, for example the interior of the Greenland ice sheet, the WFMD $XCH_4$ data are generally lower than the operational $XCH_4$ data product. Some biases still remain after quality control of the operational data, like the streak of high $XCH_4$ around 70°N and 100°E. Generally, elevated $XCH_4$ concentrations seen in the operational product for the late summer months in the Russian Taymyrsky Dolgano-Nenetsky District and the land masses between the Baffin sea and the Beaufort sea, are not real, but caused by elevated surface albedo which is not accounted for by the operational retrieval algorithm.

The cause for anomalies seen at the coastline of Greenland was recently explained by Hachmeister et al. (2022). They interpret the anomalies (100 ppb and above) caused by inaccuracies in the assumed surface elevation. This feature can be seen in the operational as well as in the WFMD $XCH_4$ data, but is

most pronounced in the operational data. These low and high methane concentration at the Greenland shoreline can be seen in the upper panels of Figure 12.

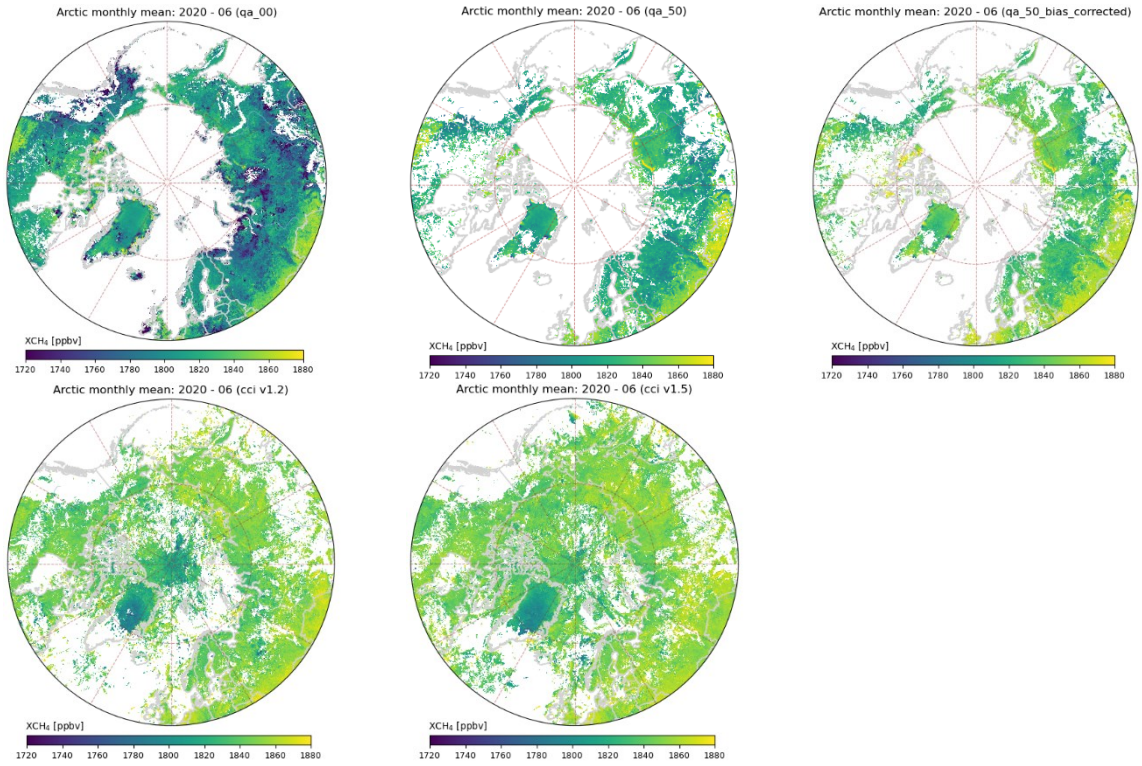


*Figure 12: Monthly mean $XCH_4$ for June 2020. Upper left: ESA $XCH_4$ without quality control, upper middle: ESA $XCH_4$ with qa_value > 0.5; upper right: $XCH_4$ qa_value > 0.5 and bias corrected. Lower left panel: WFMD $XCH_4$ version 1.2; lower right panel: WFMD $XCH_4$ version 1.5.*

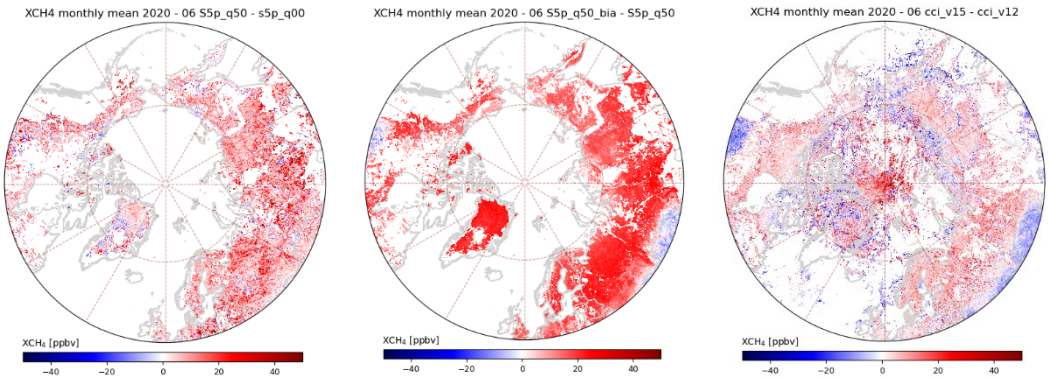


*Figure 13: Differences between monthly averaged ESA operational and ESA CCI $XCH_4$ data, illustrated for the dataset for June 2020. Left panel: differences between ESA data with (qa_value > 0.5) and without quality control; middle panel: difference between bias corrected and non-bias corrected ESA $XCH_4$ data (both with qa_value > 0.5).Right panel: differences between WFMD $XCH_4$ data version 1.5 and version 1.2*

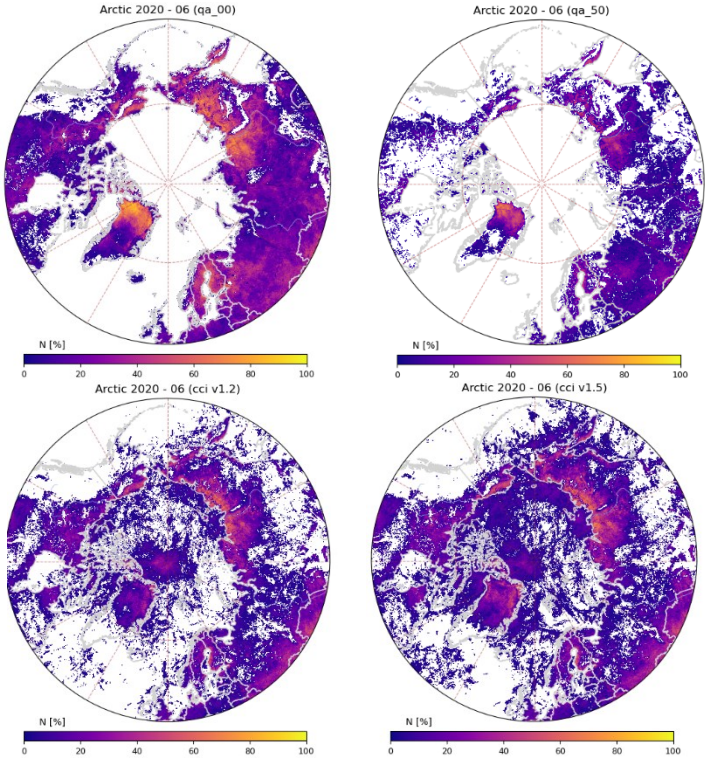


*Figure 14: Data coverage in June 2020. Upper left panel: Percentage of days with $XCH_4$ data pixels for non-quality controlled values; upper right panel: analogue for quality controlled (qa_value > 0.5) $XCH_4$ data. Lower left panel: Percentage of days with WFMD $XCH_4$ data pixels for version 1.2; Lower right panel: analogue version 1.5.*

## 2.4 Comparison of TROPOMI operational $XCH_4$ and WFMD $XCH_4$ data and timeseries for selected regions

Differences between the best operational $XCH_4$ data (bias corrected, quality controlled) and the most recent WFMD $XCH_4$ data (version 1.5) are shown in Figure 15. The upper panel shows the global overview. In addition the subsets for the Nordic countries and the Northern latitudes are shown in the lower panels.

In Norway and the Nordic boreal forest regions above 50°N, as well as some parts of the Sahara, the operational data is lower than the WFMD $XCH_4$ data. A large positive deviation is seen over the high-albedo central Greenland. In mid-latitudes, large parts of southern America, Africa and Australia the operational data is higher than the WFMD $XCH_4$ data. Histogram and correlation plots for data covering the three regional subsets is shown in Figure 16. The histograms show quality controlled, non- and bias corrected operational $XCH_4$ data as well as the WFMD $XCH_4$ data version 1.5. For the latter, the histograms for all WFMD $XCH_4$ data, as well data co-located with the operational $XCH_4$ grid cells are shown. The bias correction of the operational $XCH_4$ shifts the mean of the data by approximately +20 ppb, which results in values closer to the one of the WFMD $XCH_4$ data. While the correlation between both data sets is reasonable on a global scale, larger deviations can be seen for specific regions. For the Nordic countries the offset between the operational and the scientific values are in the order of 10-20 ppb. This is in agreement with values reported by Lorente et al., (2021). Validation of the operational $XCH_4$ data with TCOON observations at Sodankylä (Finland) (67.37°N, 26.63°E) showed a low bias of - 39.4% (-2.1% ) for un-corrected and -10.9 ppb (-0.6 %) for bias-corrected values.

At this stage, seeing the two retrievals as complementary seems to be the most reasonable approach for utilization of the Sentinel-5P $XCH_4$ data.

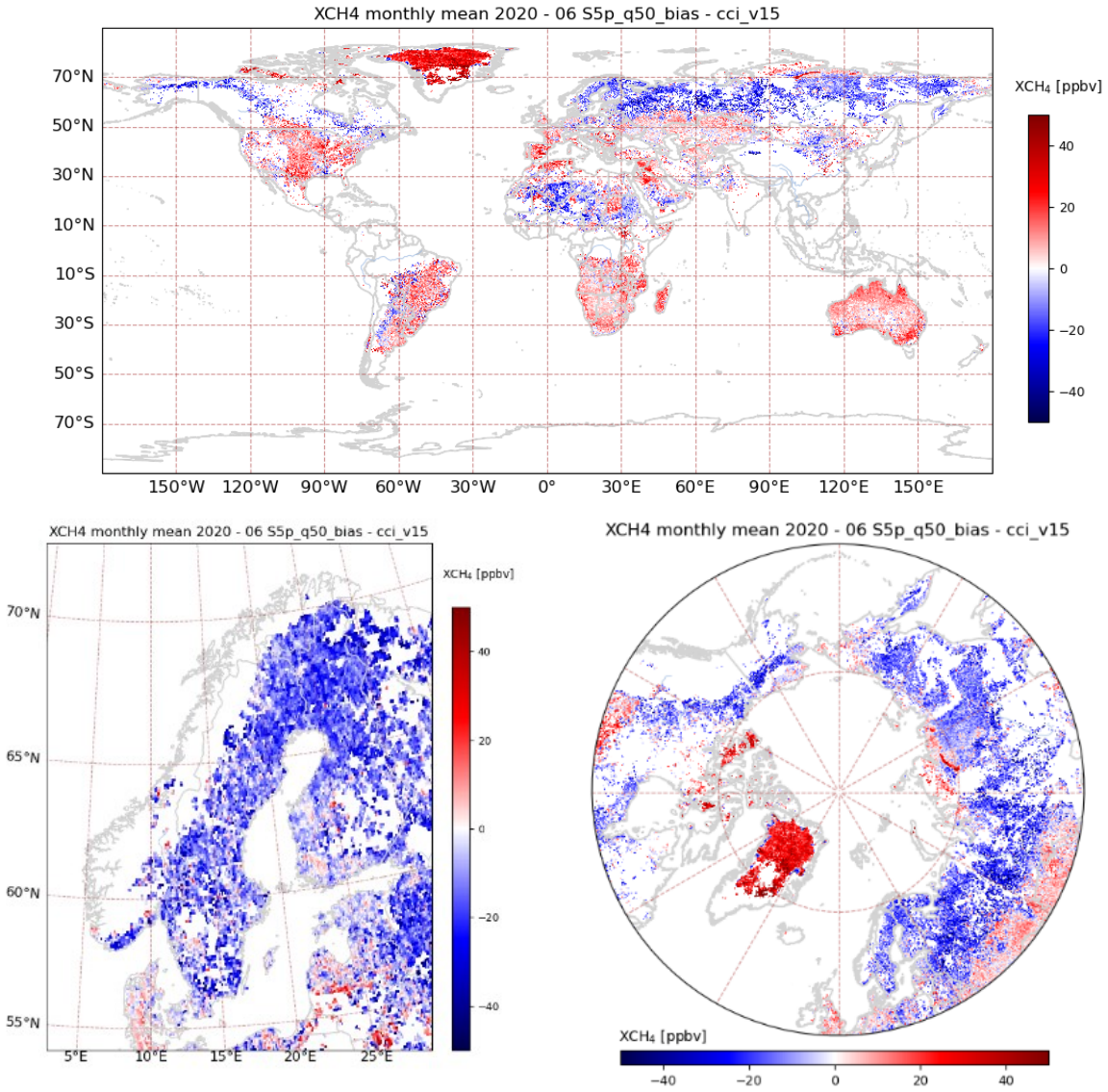


*Figure 15: Differences between the bias corrected, quality controlled operational $XCH_4$ and the WFMD $XCH_4$ data version 1.5, seen globally (upper panel), in the Nordic countries [54° N < latitude < 72° N, 3°E < longitude < 29°-E] (lower left panel) and the Arctic/Northern latitudes [> 50°N] (lower right panel).*

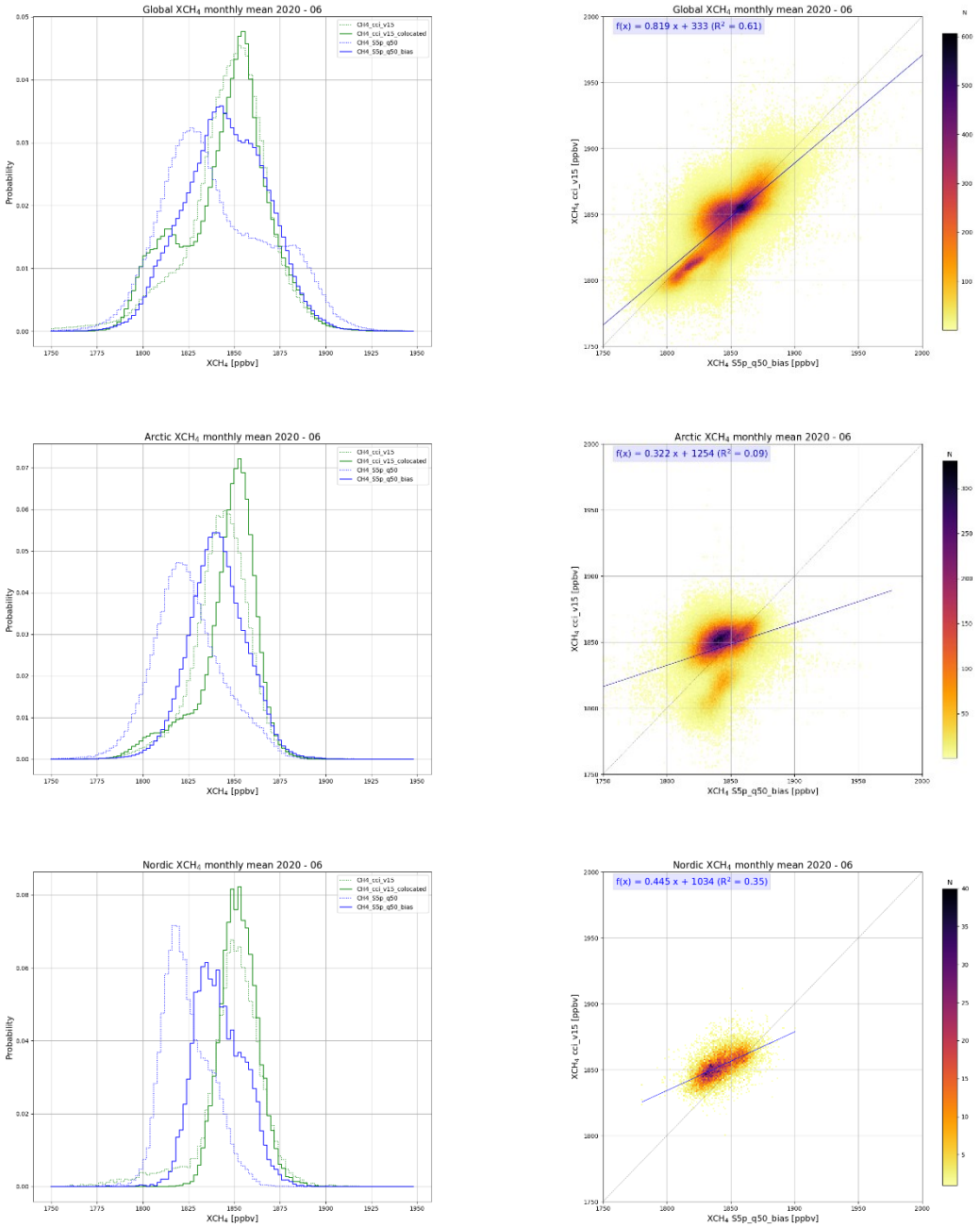


*Figure 16: Histogram and correlation plots for the bias corrected, quality controlled operational $XCH_4$ and the WFMD $XCH_4$ data version 1.5. Upper panel: global data, middle panel: data for Arctic/Northern latitudes [> 50°N], lower panel: data for the Nordic countries [54° N < latitude < 72° N, 3°E < longitude < 29°-E]. Non- and bias-corrected data operational data are shown as dashed and full blue lines in the histogram; WFMD are shown as dotted green line, WFMD data co-located with operational $XCH_4$ grid-cells are shown as full green line. The correlation plot shows the comparison of the quality controlled bias corrected operation $XCH_4$ data and the WFMD $xCH_4$ data.*

Furthermore, we show time series for monthly mean $XCH_4$ values around the two ICOS sites in Norway, i.e., the Birkenes observatory (58.4°N, 8.3°E) in Agder, the Zeppelin station (78.9°N, 11.9°E). In addition, we derive $XCH_4$ for the region around Kautokeino (69°N, 23°E**)** in Finnmark county. The latter was chosen as around this site, the operational TROPOMI data coverage is comparably high. We use data from regions around the sites, such as outlined in Figure 17. For the calculations, operational bias

corrected $XCH_4$ offline data with qa_flag > 0.5 are used, except for May to November 2018, when reprocessed (REPR) data were utilized. The WFMD $XCH_4$ data were from version 1.5.

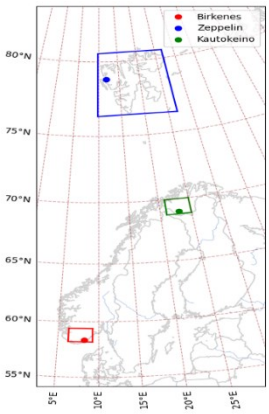


*Figure 17: Selected regions used for the calculation of monthly mean $XCH_4$.*

The estimated time series are visualized in Figure 18. Despite the large scatter and spread of the data, which will have to be investigated in more detail, two clear features stand out. $XCH_4$ is lower in the summer months, which is to be expected. The seasonality of $CH_4$ at Zeppelin and Birkenes is clearly seen in Figure 1. The $CH_4$ depends on the seasonality of the production sources (e.g. wetlands, biomass burning) and anthropogenic emissions (oil and gas installation), frequently observable outflow from Sibiria (e.g., Platt et al., 2018, Myhre et al., 2021). Furthermore, the satellite $XCH_4$ data are increasing at a rate of about 10 ppb per year. This is consistent with our methane observations both at Zeppelin and Birkenes (see Figure 1), as well as observations at other sites, and in the global mean (WMO, 2020). While an increase seems reasonable, more in-depth studies are needed once the reprocessed operational data will be made available by ESA.

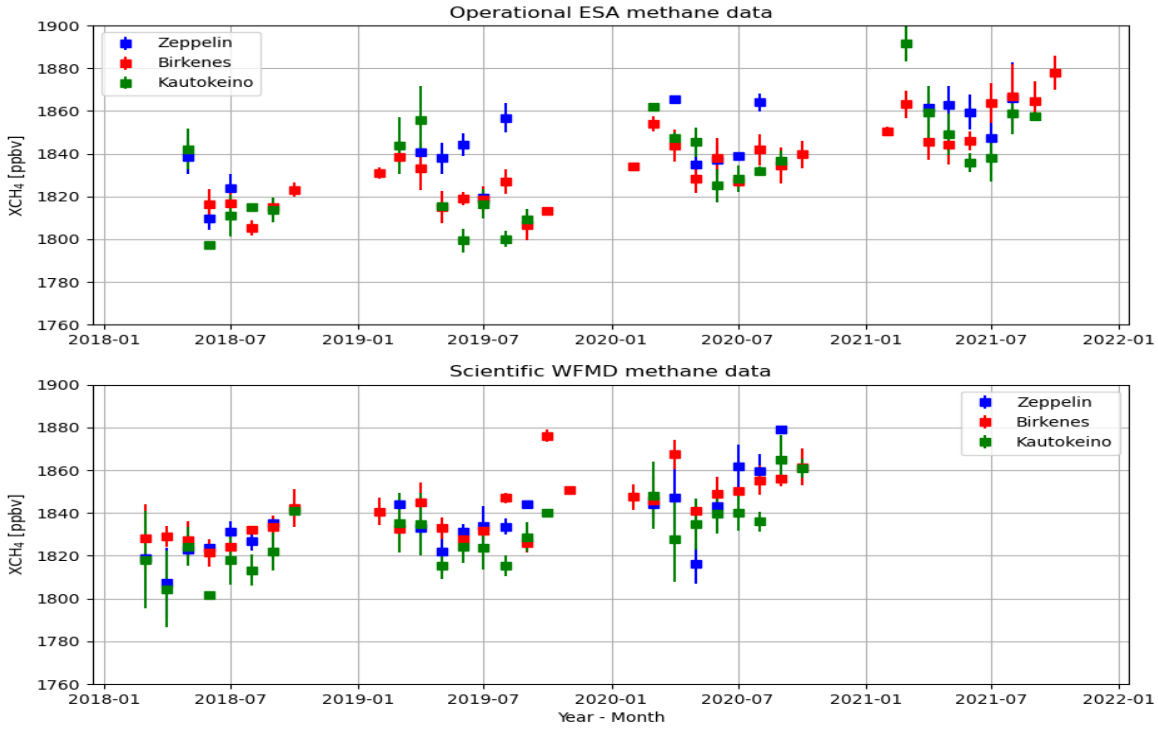


*Figure 18: Monthly mean $XCH_4$ for selected sites in Norway in 2019 and 2020.*

# 3 Task 2: Synergistic data

Task two had the primary goal of investigating and exploiting potential synergies between Sentinel products from different platforms to add value to the operational TROPOMI $CH_4$ data products.

## 3.1 Selection, acquisition, and processing of datasets

As a study period we selected the three-month period from 1 June 2020 through 30 August 2020. While the primary focus of the study is on the use of the TROPOMI $XCH_4$ product over Norwegian territory, the various datasets were initially acquired at a global scale to have the widest range of possible values for exploring relationships and fitting a statistical model.

Instead of downloading the individual datasets and subsequently processing/averaging them locally, all datasets were first processed to the desired averaging period on Google Earth Engine and then exported. All datasets were exported at 5 km spatial resolution in Plate Carree projection on WGS1984 datum (EPSG:32662). This target spatial resolution was chosen as the approximate highest resolution provided by the TROPOMI $CH_4$ product at nadir. Nearly all of the predictor variables are in principle also available at significantly higher spatial resolutions (up to 90 m), so if a good statistical model between $CH_4$ and the predictor variable can be fitted, one could in principle consider downscaling the $CH_4$ product to a somewhat finer spatial resolution, however this was outside of the scope of this study so we focused our analysis on the 5 km spatial resolution available from the original TROPOMI $CH_4$ product.

Using Google Earth Engine for this task resulted in significant time savings given the relatively large number of quite different satellite products that would have otherwise to be manually acquired, imported, and processed. In addition, the entire processing of all variables can now be very easily repeated for entirely other study periods or spatial resolutions in a very short amount of time (< 1 hour). One drawback of the described approach is that it is limited to the datasets currently available within Google Earth Engine. Other potential proxy variables would have to be manually acquired and processed in the traditional fashion.

## 3.2 TROPOMI Methane data

The operational offline methane product from S5P/TROPOMI was selected as the baseline product. Only non-bias corrected $XCH_4$ data were available on Google Earth Engine. Figure 19 shows a global map of the 3-month average methane mixing ratio for the study period. Only retrievals with a qa_value > 0.5 have been used for assembling the period average.

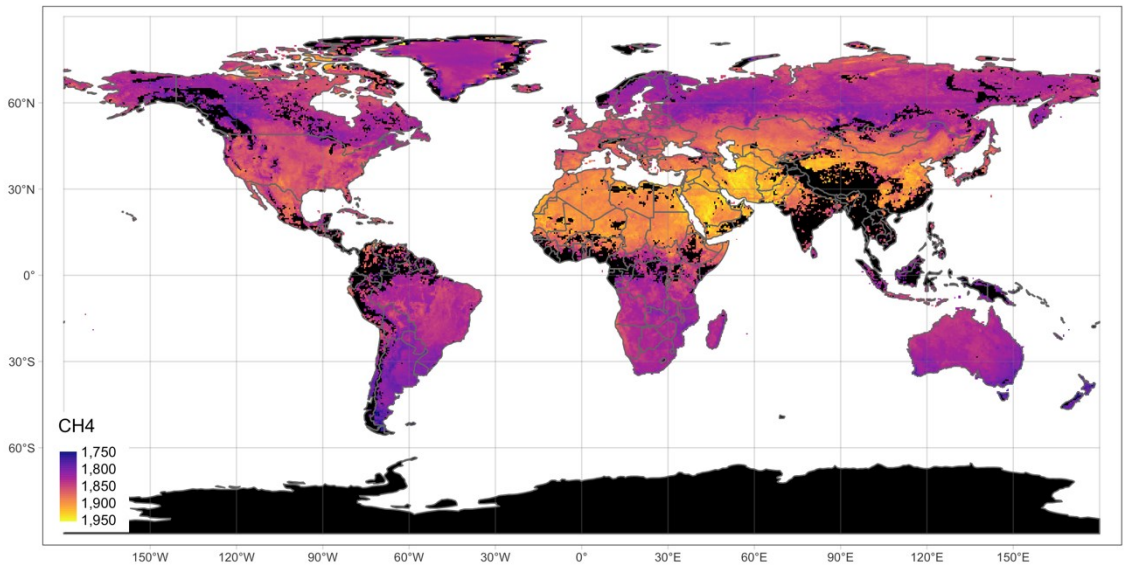


*Figure 19: Global map of $XCH_4$ from the operational TROPOMI product for the period 2020-06-01 through 2020-08-30.*

## 3.3 Candidate predictor variables

As a first potential proxy variable we selected the Normalized Difference Vegetation Index (NDVI) since it has been successfully used for very similar purposes in the past (Zhang et al. 2012) (Figure 20). Land cover was obtained from the Copernicus Global Land Service (CGLS) Dynamic Land Cover map at 100 m resolution (CGLS-LC100) (Figure 21). In contrast to many other non-dynamic land cover products, this dataset is representative specifically for the study period of July through August 2020. As an elevation dataset, the MERIT DEM was used, which is an error corrected produce based on several baseline DEMs (NASA SRTM3 DEM, JAXA AW3D DEM, Viewfinder Panoramas DEM) (Figure 22). In addition, Land Surface Temperature from the MODIS MOD11 product was used, both for daytime and night-time data and from both Terra and Aqua (Figure 23 and Figure 24). Black- and white-sky albedo in the shortwave infrared region (where the $XCH_4$ retrieval is primarily carried out) was derived from the MCD43A3 product, averaged for the entire study period (Figure 25 and Figure 26). Surface soil moisture data for the study period, were derived from the NASA-USDA Enhanced SMAP Global soil moisture dataset (Figure 27).

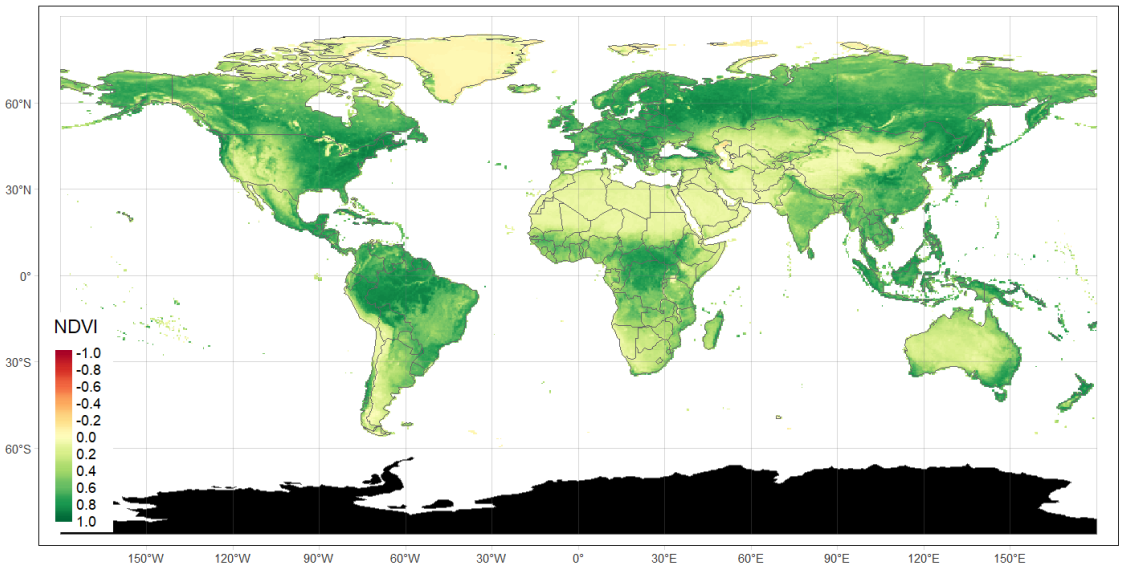


*Figure 20: Global map of average NDVI (unitless) for the study period, derived from the MODIS MOD13A1 product.*

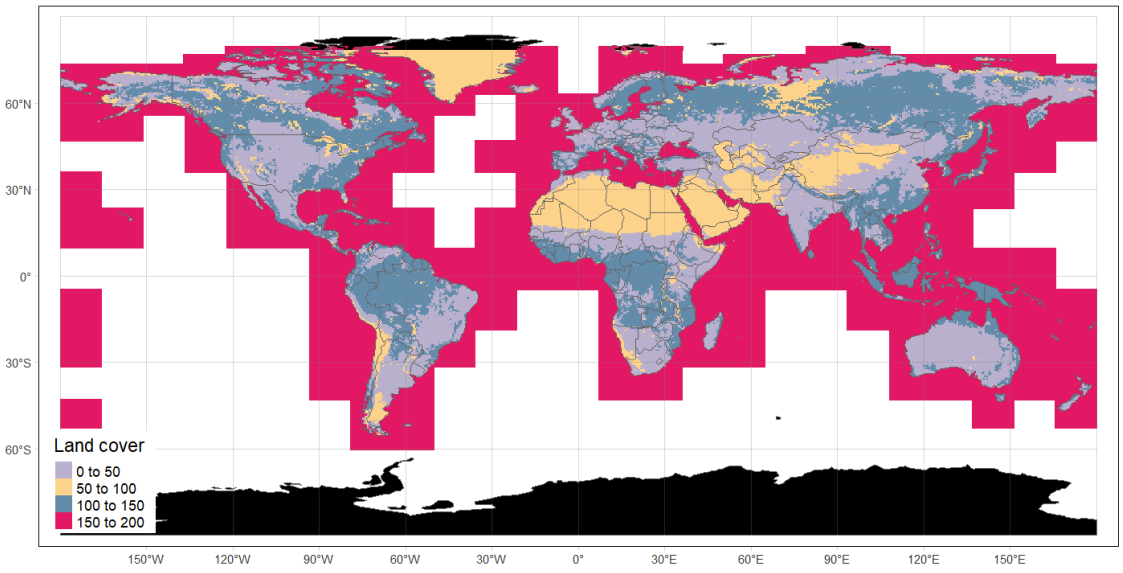


*Figure 21: Global land cover dataset for the study period derived from the CGLS-LC100 of the Copernicus Global Land Service. Note that several classes are aggregated with each other in this visualization for technical reasons – the underlying dataset provides 23 classes.*

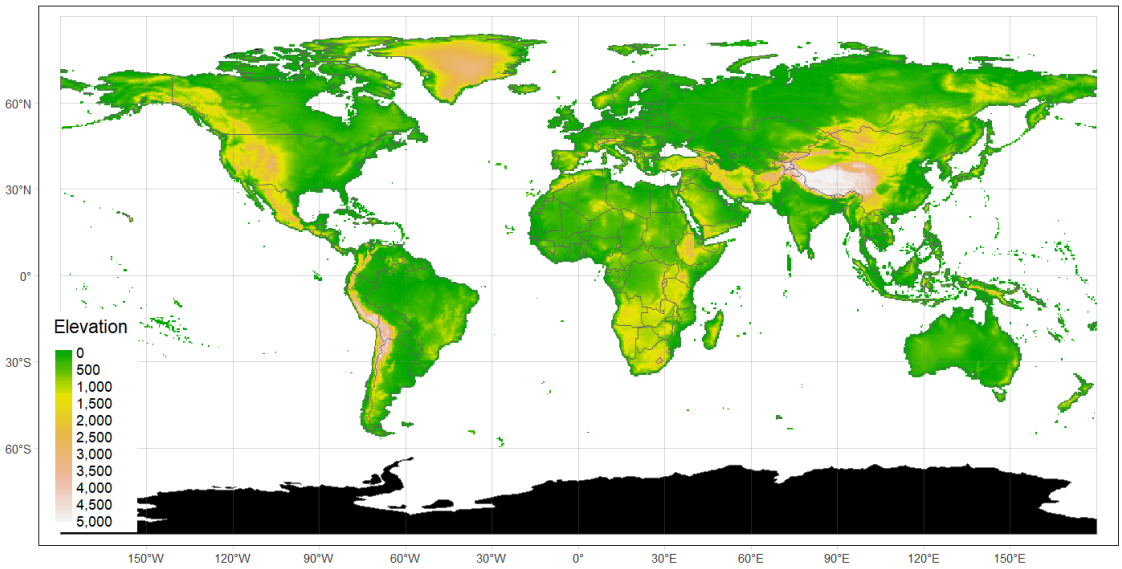


*Figure 22: Global elevation data (in meters) from the MERIT DEM (error-corrected global DEM using the NASA SRTM3 DEM, JAXA AW3D DEM, and Viewfinder Panoramas DEM as a baseline).*

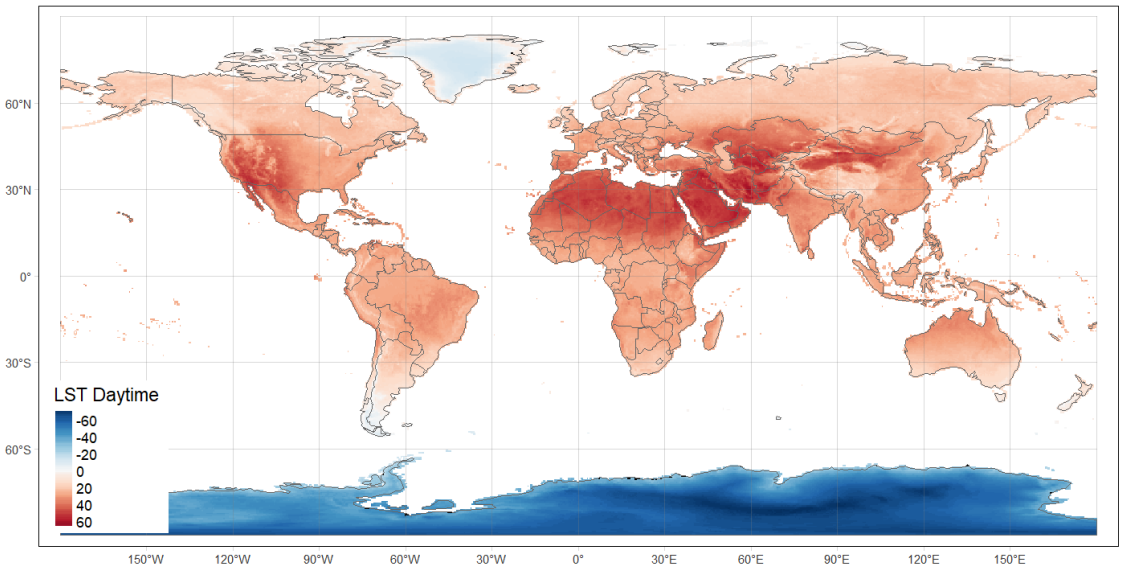


*Figure 23: Average Daytime Land Surface Temperature (in degrees Celsius) for the study period, derived from the MODIS MOD11 product.*

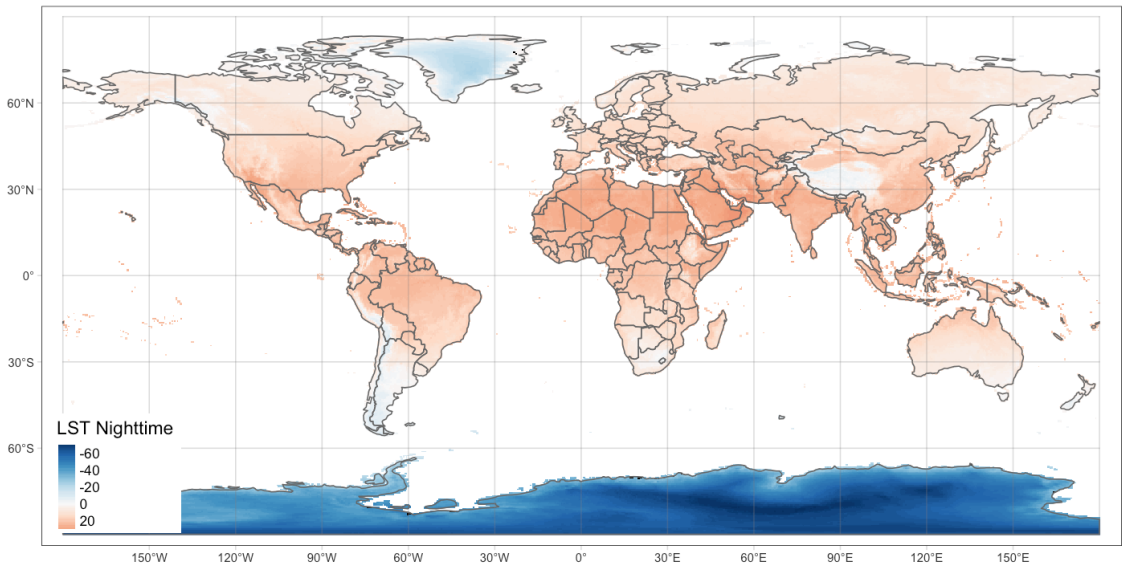


*Figure 24: Average Nighttime Land Surface Temperature (in degrees Celsius) for the study period, derived from the MODIS MOD11 product.*

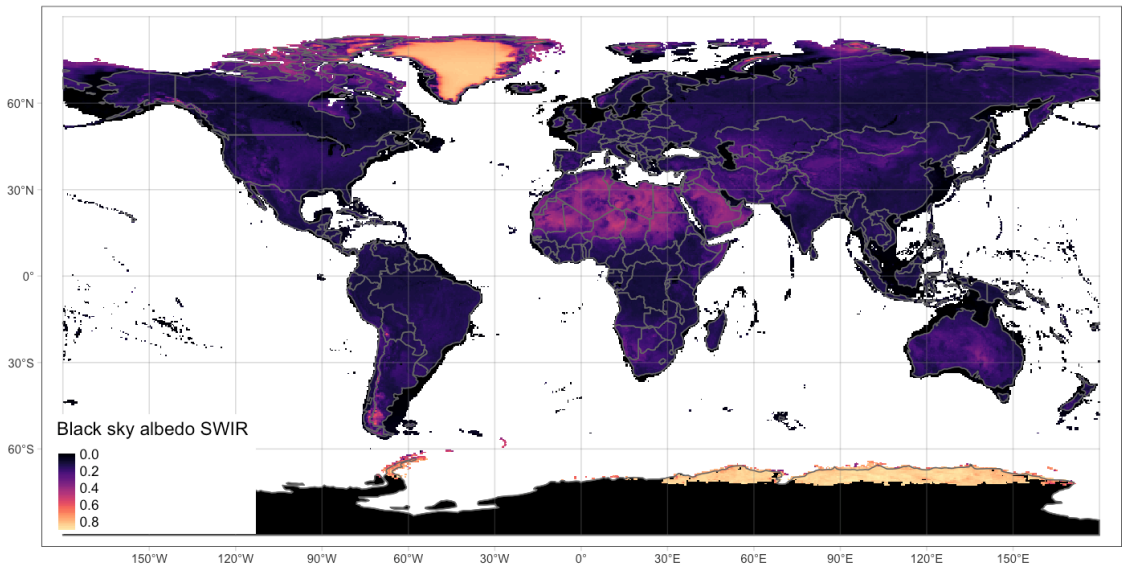


*Figure 25: Average Black Sky Albedo (unitless) in the SWIR range for the study period, derived from the MODIS MCD43A3 product.*

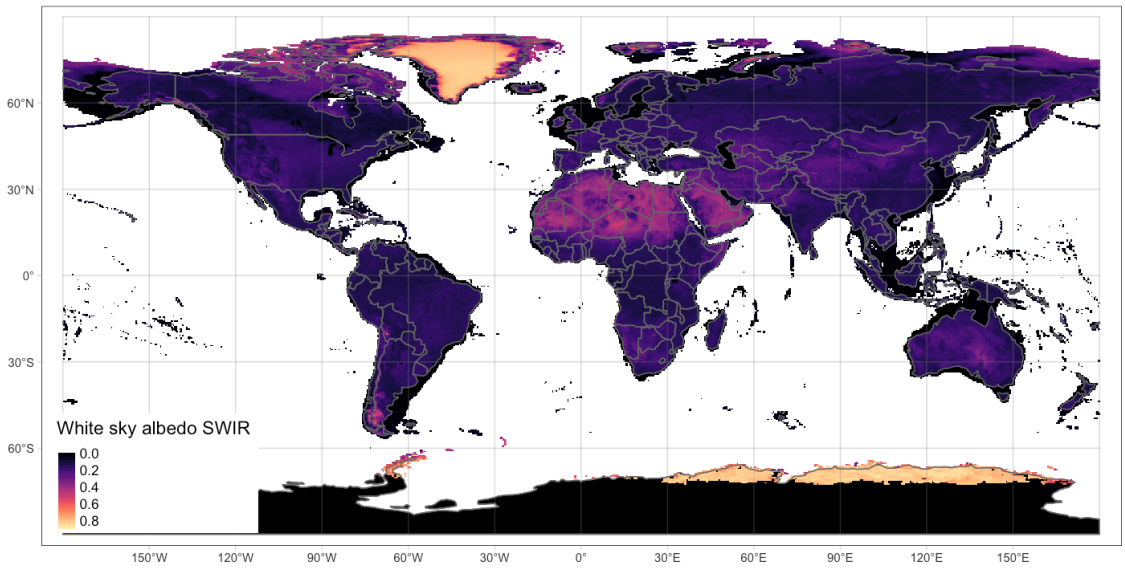


*Figure 26: Average White Sky Albedo (unitless) in the SWIR range for the study period, derived from the MODIS MCD43A3 product.*

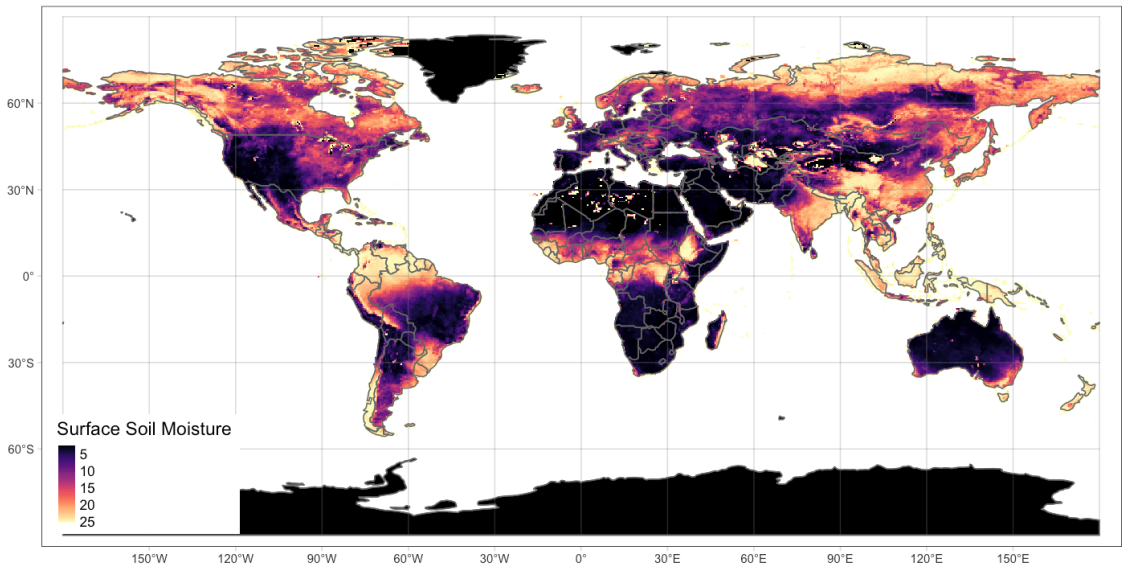


*Figure 27: Surface soil moisture data (in units of mm) for the study period, derived from the NASA-USDA Enhanced SMAP Global soil moisture dataset.*

# 4 Task 3: Statistical analysis and Machine learning

In Task 3 an initial analysis and a quantification of the spatiotemporal correlations was performed between the candidate synergy products identified in Task 2 using classical statistical techniques. Subsequently, the potential of machine learning was investigated as an alternative to further utilize the synergies between TROPOMI ($CH_4$ and other Sentinel datasets), which were identified and processed in Task 2. In the following we show an example of the correlation analysis.

The various candidate proxy variables were plotted against the $XCH_4$ data from the operational TROPOMI product. Figure 28 shows the results. NDVI shows a weak negative correlation with $XCH_4$ at the global scale. Elevation does not appear to show a relationship with $XCH_4$. Daytime LST has a moderately strong positive correlation with $XCH_4$, with nighttime LST displaying an overall similar behavior with slightly more scatter. Black-sky and white-sky SWIR albedo show a nearly identical pattern, where their relationship with $XCH_4$ shows a positive correlation between ca 0.1 and 0.3. Finally, surface soil moisture does not exhibit an obvious relationship with $XCH_4$ except for very low values, and the dataset further had significant spatial gaps over desert regions, which is why it was not further considered for the modelling step.

## 4.1 Methods

As a study period we used data between 2020-06-01 through 2020-08-30. The operational offline methane product from S5P/TROPOMI was selected as the baseline product. Figure 19 shows a global map of the 3-month average methane mixing ratio for the study period. Only retrievals with a qa_value > 0.5 have been used for assembling the period average. As predictor variables we used the variables described above, namely NDVI, elevation, daytime LST, night-time LST, and SWIR white-sky and black-sky albedo (see Figure 20 through Figure 26). The land cover predictor was initially included in the model but was found to be unsuitable due to its categorical nature, which caused both unnatural spatial artefacts in the prediction map as well as lowered the prediction accuracy substantially. Surface soil moisture was evaluated as well but since it included no data over desert areas, which would in turn allow no $XCH_4$ prediction in these areas, and since its predictor importance estimated by the RF model was very low, it was excluded from further analysis.

The model training was carried out at the global scale in order to provide as much information to the ML algorithm as possible and to ensure that the potential value range for each variable is covered. All global datasets were aggregated to 25 km spatial resolution for reducing the computational expense required for the model training. In addition, artificial gaps where introduced in the training dataset to hold back observed TROPOMI data for testing against the prediction and to thus allow an unbiased validation and to evaluate the model independent of any overfitting issues. A Random Forest (RF) model was subsequently trained based on the training dataset with artificial gaps using the “ranger” package from the R programming environment (Wright and Ziegler 2017).

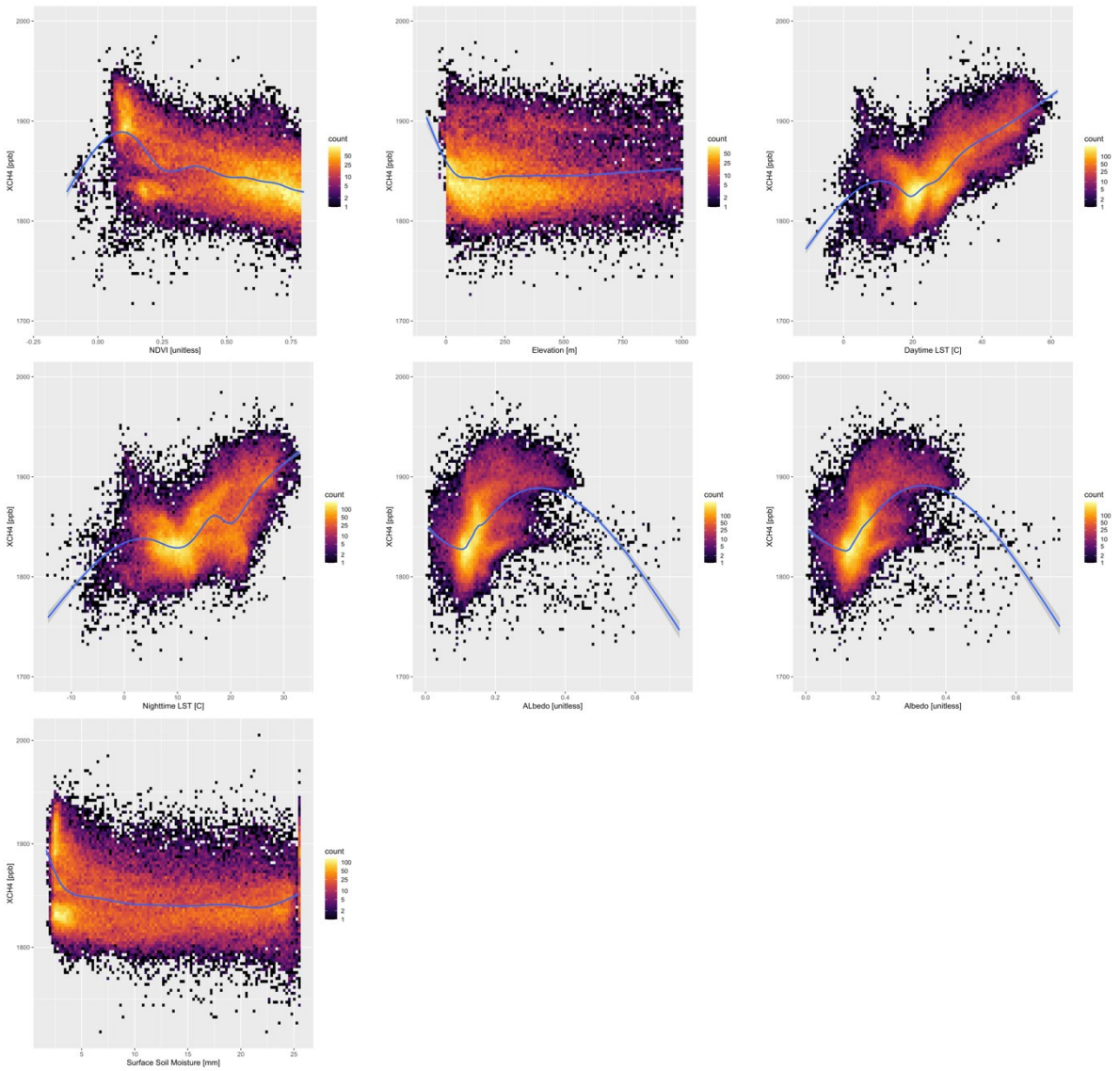


*Figure 28: Scatterplots showing the relationships between the various candidate proxy variables and TROPOMI $XCH_4$. For clarity, individual data points are not shown but they are aggregated into bins, where the colour indicates the number of data pairs falling into each bin (note the logarithmic colour scale). The blue line indicates a Loess fit to the data. Note that the land cover dataset was not plotted here since it has discrete classes rather than continuous numerical values such as the rest of the candidate proxy variables.*

## 4.2 Results

Using the trained RF model we can predict the $XCH_4$ level at any location where we have information from all predictor variables, i.e. we are able to fill gaps in the original TROPOMI-measured $XCH_4$ dataset. In Figure 29 it is illustrated how this looks in practice. The model is able to fill both small and large spatial gaps in the data and the prediction provide overall realistic spatial patterns. One exception is the center of the Greenland ice sheet where the predictions appear significantly too low compared to the measured values, and this is likely a result of extreme values in the predictor variables over this large glaciated surface.

Figure 30 shows the importance of the predictor variables as estimated by the RF algorithm. The results indicate that by the far the most important variable for predicting $XCH_4$ in this case study is the daytime LST. With quite some distance this is followed by night-time LST and white-sky albedo. NDVI, which has been exclusively used for example by Zhang et al (2012) for gap-filling and downscaling $XCH_4$, ranks only in fourth position in our case study. Black-sky albedo and elevation have the lowest importance scores. The latter is not too surprising given that the TROPOMI $XCH_4$ retrieval is not carried out over mountainous terrain, so range of elevation over which $XCH_4$ is actually retrieved is relatively low.

The RF model derived at the global scale can be readily applied for regional studies at higher spatial resolution. This is shown in Figure 31, where the global model was used to predict $XCH_4$ over the entire area of Norway. In principle the spatial patterns shown here look reasonably realistic, however given the lack of training data in mountainous areas, the $XCH_4$ predictions by the RF model for large parts of Norway must be treated with substantial caution.

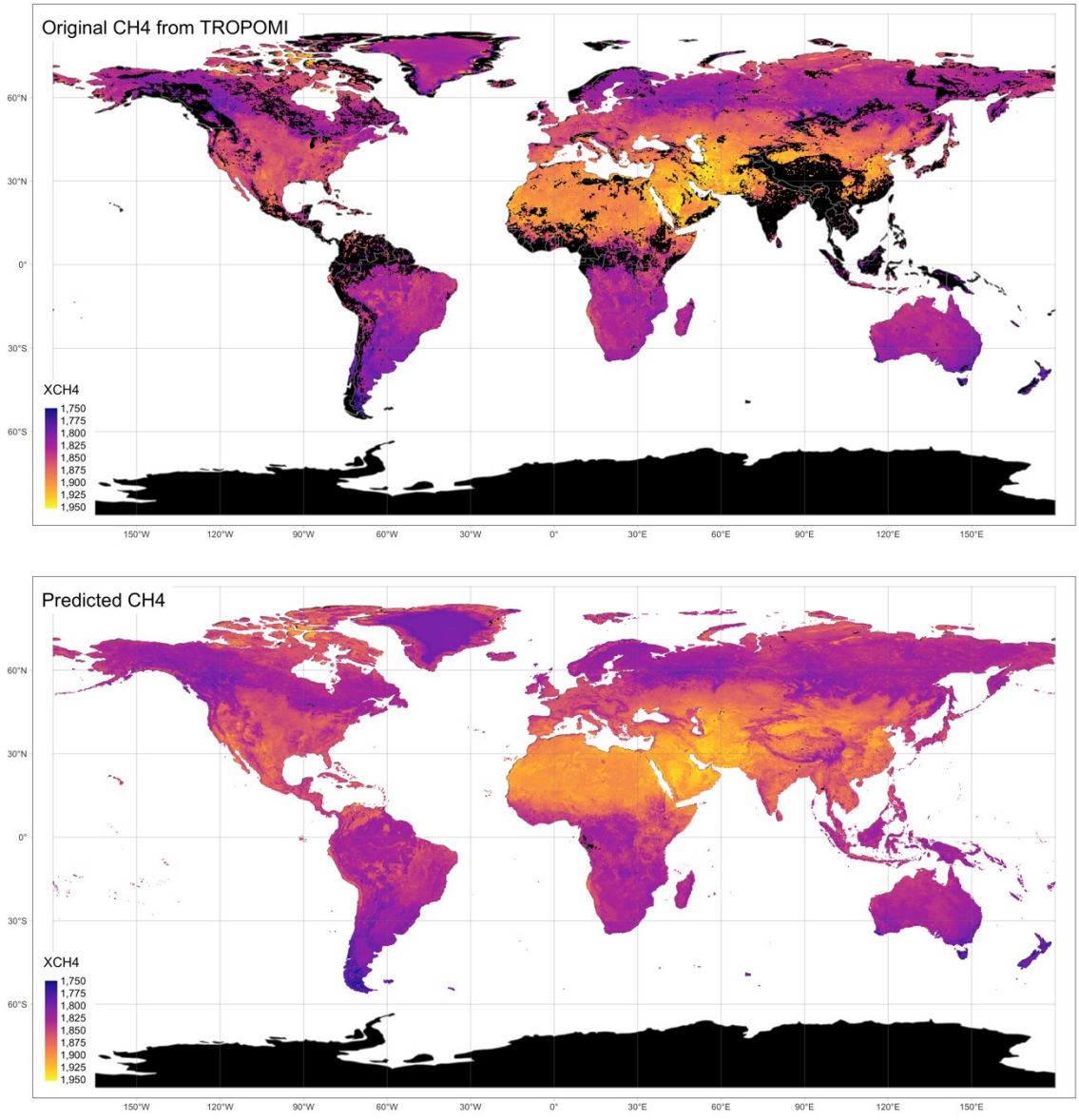


*Figure 29: Original average $XCH_4$ from TROPOMI for the period 2020-06-01 through 2020-08-30 (top panel) and gap-filled $XCH_4$ dataset for the same period, predicted using an RF model with the predictor variables NDVI, elevation, daytime LST, nighttime LST, black-sky SWIR albedo, and white-sky SWIR albedo.*

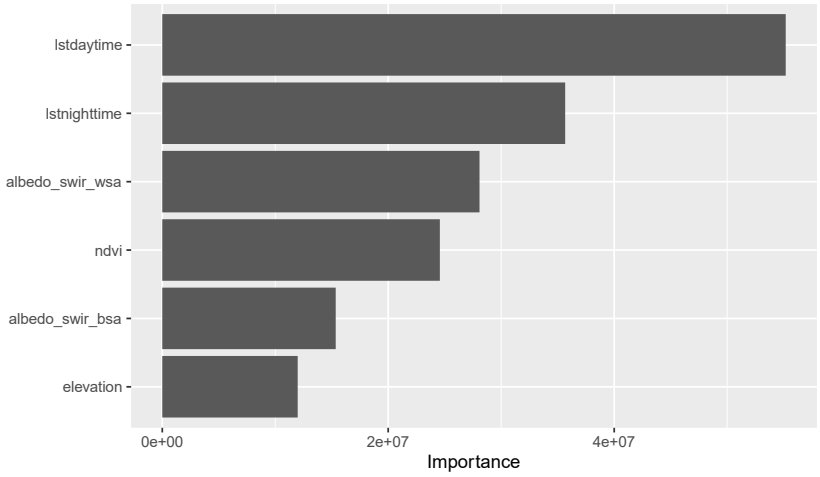


*Figure 30: Variable importance of the trained global RF model.*

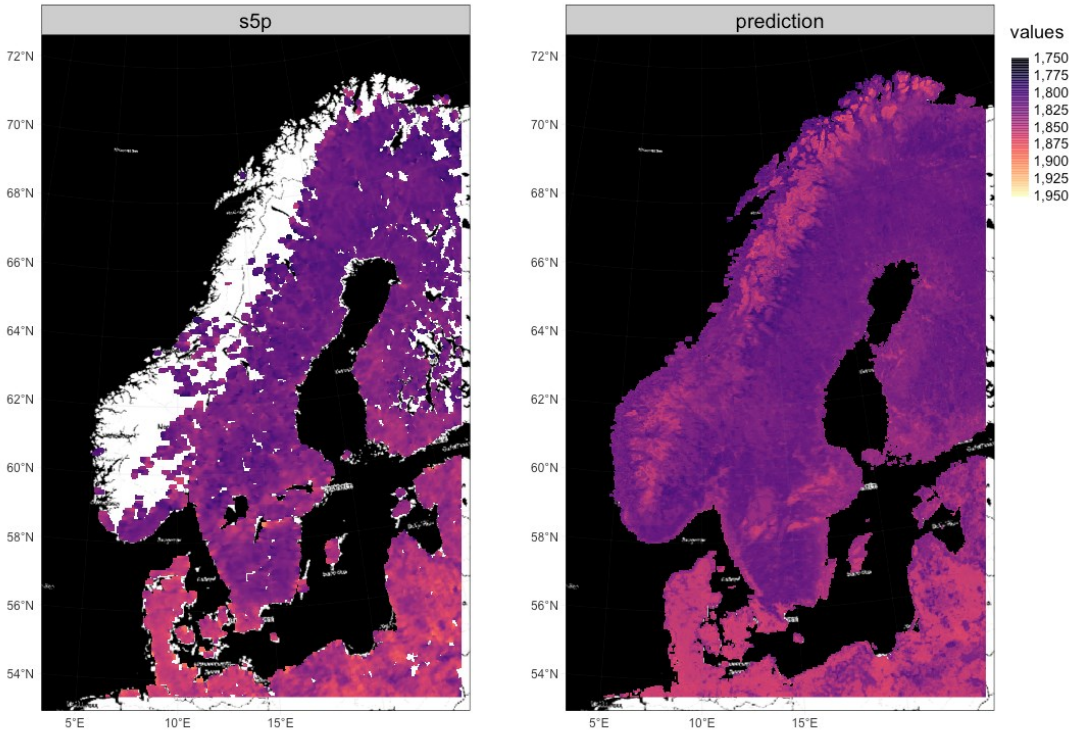


*Figure 31: Original S5P/TROPOMI $XCH_4$ retrievals over Norway (left panel) and RF-modeled $XCH_4$ (right panel). This analysis applies the RF model derived at the global scale (25 km aggregated data) at a spatial resolution of 5 km.*

The overall prediction accuracy of the RF model was estimated by introducing artificial “gaps” in the datasets (see Figure 32). This allows for a direct comparison between predicted $XCH_4$ value by the RF model and TROPOMI-observed $XCH_4$ value (where the latter was not part of the training dataset). Such a direct validation of the prediction accuracy can be found in Figure 33, which shows a scatterplot of the RF-predicted values in the artificial gaps plotted against the original true S5P/TROPOMI retrievals in those gaps, which were not used for training the model.

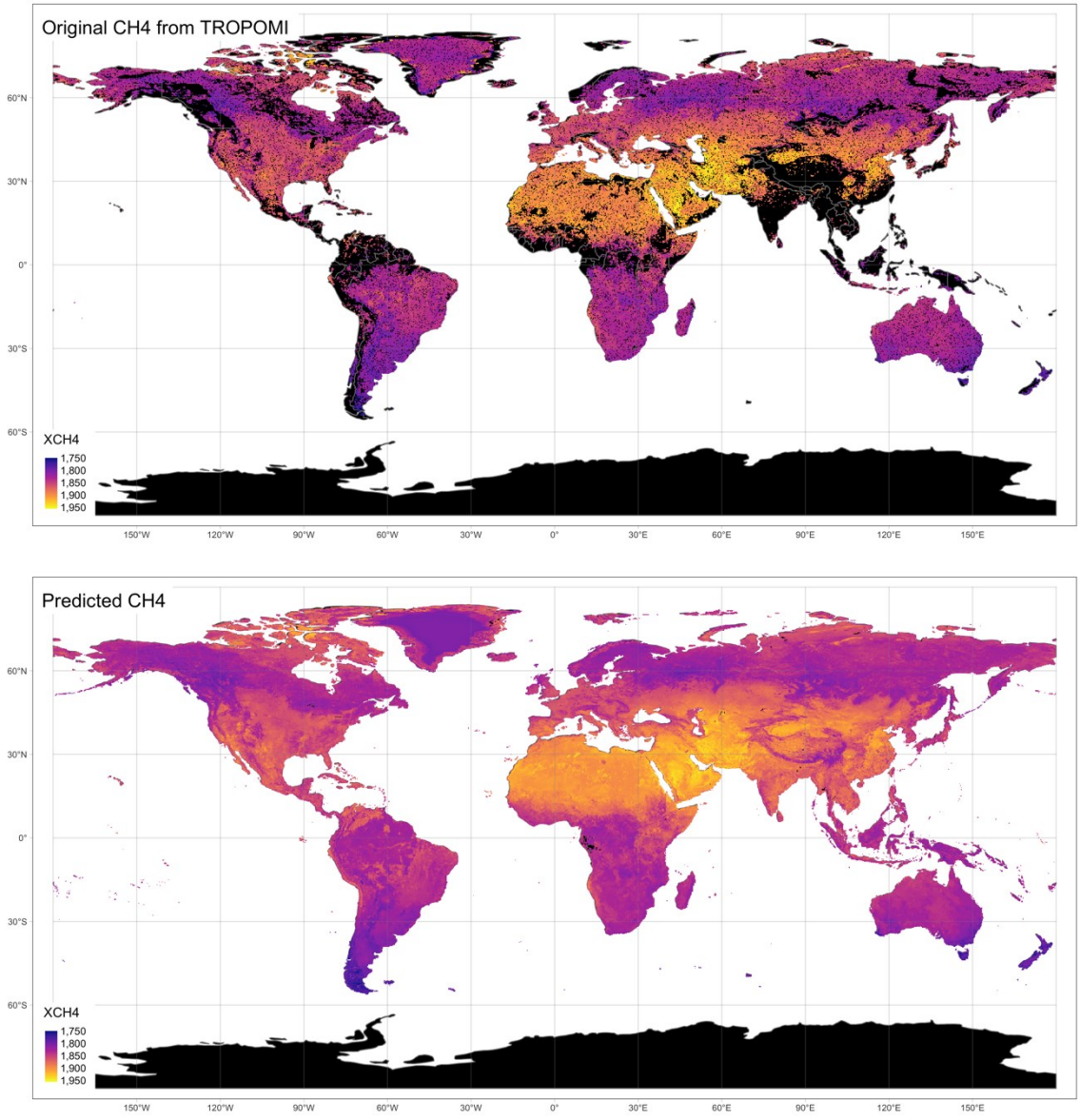


*Figure 32: Same as Figure 29, but with artificially introduced "gaps" introduced in the original $XCH_4$ dataset from TROPOMI, which can be used to quantify the prediction accuracy of the RF model.*

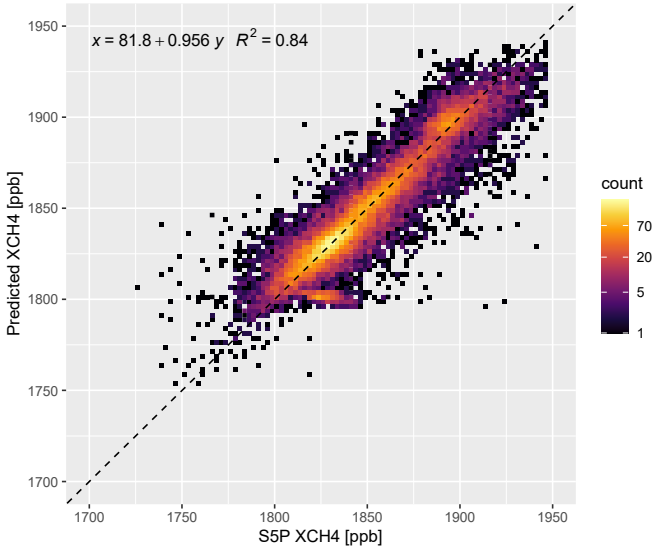


*Figure 33: Scatterplot of RF-predicted $XCH_4$ values against "true" observed $XCH_4$ values as measured by S5P/TROPOMI. In order to avoid overplotting the individual data points were binned where the colour of each bin indicates the number of data points in it (note the logarithmic colour scale).*

*Table 2: Summary statistics of the data shown in Figure 33.*

| Metric | Value |
|---|---|
| Mean error [ppb] | 0.53 |
| Standard Deviation [ppb] | 13.16 |
| Mean Absolute Error [ppb] | 8.88 |
| Root Mean Squared Error [ppb] | 13.17 |
| Regression: Intercept [ppb] | 81.80 |
| Regression: Slope [unitless] | 0.96 |
| $R^2$ [unitless] | 0.84 |

In addition to Figure 33, the modelling accuracy can further be evaluated with the metrics given in Table 2. It shows that the Root Mean Squared Error (RMSE) as a metric that is generally easily interpretable and combines both systematic and random error has a value of 13.2 ppb. Furthermore, the Table indicates a slope of the data very close to unity (0.96). Overall, these results indicate that the RF-model has a very good capability of filling small gaps in the data. With an $R^2$ value of 0.84 the model is able to explain 84% of the total variance.

It should be noted, however, that these validation results can only provide information about the modelling accuracy in areas that match the general $XCH_4$- and predictor-characteristics of those regions where actual S5P/TROPOMI retrievals are available. While the results look overall promising, it should be noted that ML algorithms can typically only predict well for conditions that they have been previously trained for. This has an implication on filling gaps over mountainous areas since the operational TROPOMI $XCH_4$ product is typically not retrieved over mountain areas. As such, for these regions the RF model implicitly extrapolates functional relationships with the predictor variables from other regions where data is available. This can result in erroneous estimates over such areas, which are difficult to assess given the lack of other observational data. One possibility to overcome this issue would be to exploit the better coverage over mountain areas of the WFMD $XCH_4$ product, however such a comparison has to be carried out with caution since the actual retrieval algorithms are quite

different, and the two products are subject to significant systematic differences and random error. As such, in a comparison along these lines it would be challenging to disentangle the actual RF model error from inter-product differences.

# 5 Summary and conclusions

The main goal of this feasibility study was to evaluate the possibility of adding value to the Sentinel-5P TROPOMI methane product over Norway and the Arctic through synergistic use of relevant observations from other Sentinel satellites and machine learning. For this, we first assessed the data availability of operational TROPOMI and the WFMD $XCH_4$ products (version 1.2 and 1.5) over the northern hemisphere, the Nordic countries and the Arctic/Northern latitudes. Effects of quality control and bias correction of the operational data were analysed. The bias correction corrects the $XCH_4$ underestimation for low albedo values, and reduces the overestimation for high albedo values over desert areas. It thus makes the operational data more comparable to the most recent WFMD $XCH_4$ product. For the Nordic countries and the boreal forest region in Russia, the operational data are about 10-20 ppb lower than the scientific $XCH_4$ values. A main caveat of the operational ESA $XCH_4$ data is its poor coverage over Norway, and that there are no data available over the ocean. Due to the low data coverage, the initially planned additional filtering to generate improved seasonal $CH_4$-maps did not seem useful to be performed within the STEPS projects. Time series for selected regions around Birkenes, Karasjok, and Svalbard show seasonal variations, with lower values in summer, and a general increase throughout the four-year period. This is consistent with the strong increase seen in the $CH_4$-levels in our observations both at Zeppelin and Birkenes as well as observations at other sites, and in the global mean (WMO, 2020).

We further investigated potential synergies between satellite products from other platforms to add value to the operational TROPOMI $CH_4$ data products. Various candidate predictor variables from other satellite instruments were acquired and the relationship of this data with the operational $XCH_4$ product was evaluated. Subsequently, a random forest machine learning algorithm was trained and applied in order to estimate, solely using the predictor variables, $XCH_4$ values in areas were no TROPOMI data is available. As predictor variables we used NDVI, land cover, elevation, daytime- and night-time land surface temperatures, black- and white sky albedo and surface soil moisture data. The results indicate that by the far the most important variable for predicting $XCH_4$ in this case study is daytime LST, followed by night-time LST and white-sky albedo. NDVI, which has been exclusively used for example by Zhang et al (2012) for gap-filling and downscaling $XCH_4$, ranks only in fourth position in our case study. Our results indicate that the RF-model has a very good capability of filling small gaps in the data. The model is able to predict $XCH_4$ with an $R^2$ value of 0.84 and an RMSE/standard deviation of 13 ppb. For reference, the latter is about the same (summer) or significantly lower (winter) than the standard deviation between the operational and WFMD $XCH_4$ products (Schneising et al. 2019). It should be noted, however, that ML algorithms can typically only predict well for conditions that they have been previously trained for. This has implications on filling gaps over mountainous areas in Norway since the operational TROPOMI $XCH_4$ product is typically not retrieved over mountain areas. Due to the lack of directly comparable reference data, the accuracy of the machine learning model could not be quantitatively evaluated over such regions. However, a qualitative comparison with the WFMD product indicates that the predicted values over Norway are likely biased high and show some unrealistic spatial patterns. We recommend restricting the use of ML-based gap filling to areas for which satellite retrievals are generally carried out so that sufficient training information is available.

The WFMD $XCH_4$ data shows better coverage than the operational data, including data over the ocean, but these data are only available until the end of 2020, and are not provided in near-real-time. Reprocessing of the operational data was announced for 2022, and it is expected that the upcoming version will have better data coverage. Nevertheless, it remains to be seen which improvements will

be made during the re-processing and how this will affect availability and quality of the data over the Norwegian territory, Northern latitudes and the Arctic. Meanwhile seeing these two versions as complementary – as mini-ensemble, seems to be the most reasonable approach for utilization of the Sentinel-5P $XCH_4$ data.

To support NILU's monitoring activities, follow up investigations of the methane data in the Northern latitudes (> 50°N) seem highly valuable. This will allow us to better understand the anthropogenic and natural source regions, and their potential influence on the observations at the Zeppelin and Birkenes monitoring stations. Particularly interesting seems to be using TROPOMI data to estimate the methane emissions e.g. in Russia, which regularly affect the Zeppelin-observations, for example, applying the divergence method recently published by Liu at el. (2021), which they applied to derive annual $CH_4$-emission over the Permian Basin in the USA. The fluxes derived solely from satellite may then be compared to those obtained from a full inversion made within the ReGAME project. With regard to machine learning, the initial results from this study appear very promising and further work could evaluate more advanced algorithms such as XGBoost and possibly the use of additional predictor variables with regard to their potential to increase the prediction accuracy. Additional work on validating the output from the ML-model is further recommended. Besides continuing work with Sentinel-5P, the use of satellites with higher spacial resolution seems a valuable step forwards to quantify large point sources in the North, which influence our measurements. Methane retrieval from non-commercial freely available data, like Sentinel-2 (Varon et al., 2021), PRISMA (Guanter et al., 2021), the upcoming MethaneSAT (Launch ~ 2022, https://www.methanesat.org/) and the CarbonMapper (Launch ~ 2023, https://carbonmapper.org/) are of particular interest in this context.

# 6 References

Groot Zwaaftink, C. D., Henne, S., Thompson, R. L., Dlugokencky, E. J., Machida, T., Paris, J.-D., Sasakawa, M., Segers, A., Sweeney, C., and Stohl, A.: Three-dimensional methane distribution simulated with FLEXPART 8-CTM-1.1 constrained with observation data, Geosci. Model Dev., 11, 4469–4487, https://doi.org/10.5194/gmd-11-4469-2018, 2018.

Guanter, L., Irakulis-Loitxate, I., Gorroño, J., Sánchez-García, E., Cusworth, D.H., Varon, D.J., Cogliati, S., and Colombo, R.: Mapping methane point emissions with the PRISMA spaceborne imaging spectrometer, Remote Sens. Environ., 265, 112671, https://doi.org/10.1016/j.rse.2021.112671, 2021.

Hachmeister, J., Schneising, O., Buchwitz, M., Lorente, A., Borsdorff, T., Burrows, J. P., Notholt, J., and Buschmann, M.: On the influence of underlying elevation data on Sentinel-5 Precursor satellite methane retrievals over Greenland, Atmos. Meas. Tech. Discuss. [preprint], https://doi.org/10.5194/amt-2022-102, in review, 2022.

Hasekamp, O., Lorente, A.,Hu, H., Butz, A., aan de Brugh, J., and Landgraf, J.: Algorithm Theoretical Baseline Document for Sentinel-5 Precursor Methane Retrieval, SRON ref: SRON-S5P-LEV2-RP-001, issue 2.3.1, 2021-10-27, https://sentinel.esa.int/documents/247904/2476257/Sentinel-5P-TROPOMI-ATBD-Methane-retrieval, 2021 (last assessed 29 March 2022).

Heiskanen, J., Brümmer, C., Buchmann, N., Calfapietra, C., Chen, H., Gielen, B., Gkritzalis, T., Hammer, S., Hartman, S., Herbst, M., Janssens, I. A., Jordan, A., Juurola, E., Karstens, U., Kasurinen, V., Kruijt, B., Lankreijer, H., Levin, I., Linderson, M., Loustau, D., Merbold, L., Myhre, C. L., Papale, D., Pavelka, M., Pilegaard, K., Ramonet, M., Rebmann, C., Rinne, J., Rivier, L., Saltikoff, E., Sanders, R., Steinbacher, M., Steinhoff, T., Watson, A., Vermeulen, A. T., Vesala, T., Vítková, G., and Kutsch, W.: The Integrated Carbon Observation System in Europe, B. Am. Meteorol. Soc., https://doi.org/10.1175/BAMS-D-19-0364.1, 2022.

Hu, H., Hasekamp, O., Butz, A., Galli, A., Landgraf, J., Aan de Brugh, J., Borsdorff, T., Scheepmaker, R., and Aben, I.: The operational methane retrieval algorithm for TROPOMI, Atmos. Meas. Tech., 9, 5423–5440, https://doi.org/10.5194/amt-9-5423-2016, 2016.

Hu, H., Landgraf, J., Detmers, R., Borsdorff, T., Aan de Brugh, J., Aben, I., A., Butz, A., and Hasekamp, O.: Toward global mapping of methane with TROPOMI: First results and intersatellite comparison to GOSAT. Geophys. Res. Lett., 45, 3682–3689, https://doi.org/10.1002/2018GL077259, 2018.

Kylling, A., Stebel, K., Fjæraa, A. M., and Schneider, P.: Fjernmåling av metanutslipp ved bruk av Sentinel-5P: en mulighetsstudie, NILU rapport, 9/2021, Kjeller, NILU. https://hdl.handle.net/11250/2756989, 2021.

Landgraf, J., Butz, A., Hasekamp, O., Hu, H., and aan de Brugh, J.: Sentinel 5 L2 Prototype Processors, Algorithm Theoretical Baseline Document: Methane Retrieval, SRON-ESA-S5L2PPATBD-001-v3.1-20190517-CH4, SRON Netherlands Institutefor Space Research, Utrecht, the Netherlands, 2019.

Landgraf, J., Lorente, A., Langerock, B., and Sha, M.K., S5P Mission Performance Centre Methane [L2__CH4___] Readme. source: ref: Version V02.03.01, S5P-MPC-SRON-PRF-CH4; date: 2021-11-17. https://sentinel.esa.int/documents/247904/3541451/Sentinel-5P-Methane-Product-Readme-File, 2021, (last assessed 29 March 2022).

Lorente, A., Borsdorff, T., Butz, A., Hasekamp, O., aan de Brugh, J., Schneider, A., Wu, L., Hase, F., Kivi, R., Wunch, D., Pollard, D. F., Shiomi, K., Deutscher, N. M., Velazco, V. A., Roehl, C. M., Wennberg, P. O., Warneke, T., and Landgraf, J.: Methane retrieved from TROPOMI: improvement of the data product and validation of the first 2 years of measurements, Atmos. Meas. Tech., 14, 665–684, https://doi.org/10.5194/amt-14-665-2021, 2021.

Liu, M., van der A, R., van Weele, M., Eskes, H., Lu, X., Veefkind, P., de Laat, J., Kong5, H., Wang , J., Sun, J., Ding, J., Zhao, Y., and Weng, H., A new divergence method to quantify methane emissions using observations of Sentinel-5P TROPOMI. Geophysical Research Letters, 48, e2021GL094151. https://doi.org/10.1029/2021GL094151, 2021.

Myhre, C. L., Svendby, T. M., Hermansen, O., Lunder, C.R., Platt, S. M., Fiebig, M., Fjæraa, A. M., Hansen, G. H.,Schmidbauer, N., Krognes, T., and Walker, S.-E.: Monitoring of greenhouse gases and aerosols at Svalbard and Birkenes in 2020. Annual report, NILU report, 22/2021, NILU, Kjeller. https://hdl.handle.net/11250/2832204, 2021.

Nisbet, E. G., Manning, M. R., Dlugokencky, E. J., Fisher, R. E., Lowry, D., Michel, S. E., Myhre, C. Lund, Platt, S. M., Bousquet, A. P., Cain, R. B. M., France, J. L., Hermansen, O., Hossaini, R., Jones, A. E., Levin, I., Manning, A. C., Myhre, G., Pyle, J. A., Vaughn, B. H., Warwick, N. J., White, J. W. C.: Very strong atmospheric methane growth in the 4 years 2014–2017: Implications for the Paris Agreement. Global Biogeochemical Cycles, 33, 318–342. https://doi.org/10.1029/2018GB006009, 2019

Platt, S. M., Eckhardt, S., Ferré, B., Fisher, R. E., Hermansen, O., Jansson, P., Lowry, D., Nisbet, E. G., Pisso, I., Schmidbauer, N., Silyakova, A., Stohl, A., Svendby, T. M., Vadakkepuliyambatta, S., Mienert, J., and Lund Myhre, C.: Methane at Svalbard and over the European Arctic Ocean, Atmos. Chem. Phys., 18, 17207–17224, https://doi.org/10.5194/acp-18-17207-2018, 2018.

Saunois, M., Stavert, A. R., Poulter, B., Bousquet, P., Canadell, J. G., Jackson, R. B., Raymond, P. A., Dlugokencky, E. J., Houweling, S., Patra, P. K., Ciais, P., Arora, V. K., Bastviken, D., Bergamaschi, P., Blake, D. R., Brailsford, G., Bruhwiler, L., Carlson, K. M., Carrol, M., Castaldi, S., Chandra, N., Crevoisier, C., Crill, P. M., Covey, K., Curry, C. L., Etiope, G., Frankenberg, C., Gedney, N., Hegglin, M. I., Höglund-Isaksson, L., Hugelius, G., Ishizawa, M., Ito, A., Janssens-Maenhout, G., Jensen, K. M., Joos, F., Kleinen, T., Krummel, P. B., Langenfelds, R. L., Laruelle, G. G., Liu, L., Machida, T., Maksyutov, S., McDonald, K. C., McNorton, J., Miller, P. A., Melton, J. R., Morino, I., Müller, J., Murguia-Flores, F., Naik, V., Niwa, Y., Noce, S., O'Doherty, S., Parker, R. J., Peng, C., Peng, S., Peters, G. P., Prigent, C., Prinn, R., Ramonet, M., Regnier, P., Riley, W. J., Rosentreter, J. A., Segers, A., Simpson, I. J., Shi, H., Smith, S. J., Steele, L. P., Thornton, B. F., Tian, H., Tohjima, Y., Tubiello, F. N., Tsuruta, A., Viovy, N., Voulgarakis, A., Weber, T. S., van Weele, M., van der

Werf, G. R., Weiss, R. F., Worthy, D., Wunch, D., Yin, Y., Yoshida, Y., Zhang, W., Zhang, Z., Zhao, Y., Zheng, B., Zhu, Q., Zhu, Q., and Zhuang, Q.: The Global Methane Budget 2000–2017, Earth Syst. Sci. Data, 12, 1561–1623, https://doi.org/10.5194/essd-12-1561-2020, 2020.

Schneising, O., Buchwitz, M., Reuter, M., Bovensmann, H., Burrows, J. P., Borsdorff, T., Deutscher, N. M., Feist, D. G., Griffith, D. W. T., Hase, F., Hermans, C., Iraci, L. T., Kivi, R., Landgraf, J., Morino, I., Notholt, J., Petri, C., Pollard, D. F., Roche, S., Shiomi, K., Strong, K., Sussmann, R., Velazco, V. A., Warneke, T., and Wunch, D.: A scientific algorithm to simultaneously retrieve carbon monoxide and methane from TROPOMI onboard Sentinel-5 Precursor, Atmos. Meas. Tech., 12, 6771–6802, https://doi.org/10.5194/amt-12-6771-2019, 2019.

Schneising, O., Algorithm Theoretical Basis Document (ATBD) TROPOMI WFM-DOAS (TROPOMI/WFMD) $XCH_4$, ESA Climate Change Initiative “Plus” (CCI+), 12.07.2021 https://www.iup.uni-bremen.de/carbon_ghg/products/tropomi_wfmd/ atbd_wfmd.pdf (last assessed 29 March 2022).

Thompson, R. L., Sasakawa, M., Machida, T., Aalto, T., Worthy, D., Lavric, J. V., Lund Myhre, C., and Stohl, A.: Methane fluxes in the high northern latitudes for 2005–2013 estimated using a Bayesian atmospheric inversion, Atmos. Chem. Phys., 17, 3553–3572, https://doi.org/10.5194/acp-17-3553-2017, 2017.

Wright MN, Ziegler A . “ranger: A Fast Implementation of Random Forests for High Dimensional Data in C++ and R.” Journal of Statistical Software, 77(1), 1–17. https://doi.org/10.18637/jss.v077.i01, 2017.

Varon, D. J., Jervis, D., McKeever, J., Spence, I., Gains, D., and Jacob, D. J.: High-frequency monitoring of anomalous methane point sources with multispectral Sentinel-2 satellite observations, Atmos. Meas. Tech., 14, 2771–2785, https://doi.org/10.5194/amt-14-2771-2021, 2021.

Zhang, X., Jiang, H., Zhou, G., Xiao, Z., and Zhang, Z.: Geostatistical interpolation of missing data and downscaling of spatial resolution for remotely sensed atmospheric methane column concentrations. International Journal of Remote Sensing, 33(1), 120–134. https://doi.org/10.1080/01431161.2011.584078, 2012.

# Appendix A

# Monthly mean $XCH_4$ for the Nordic countries

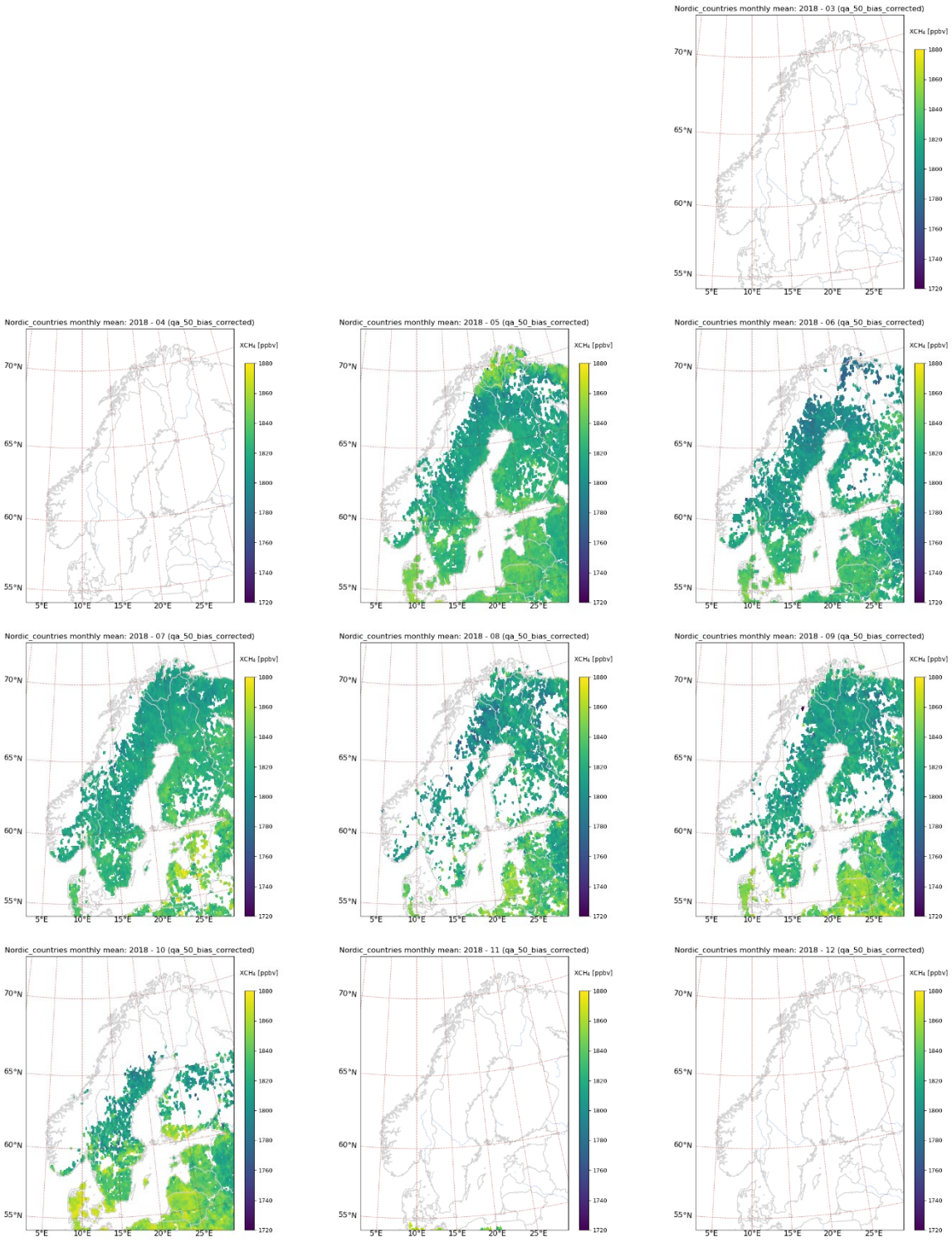


*Figure A1. Operational bias corrected $XCH_4$ for the year 2018 offline (OFFL – March, April, December) and reprocessed (RPRO – May - November) data with qa_value > 0.5.*

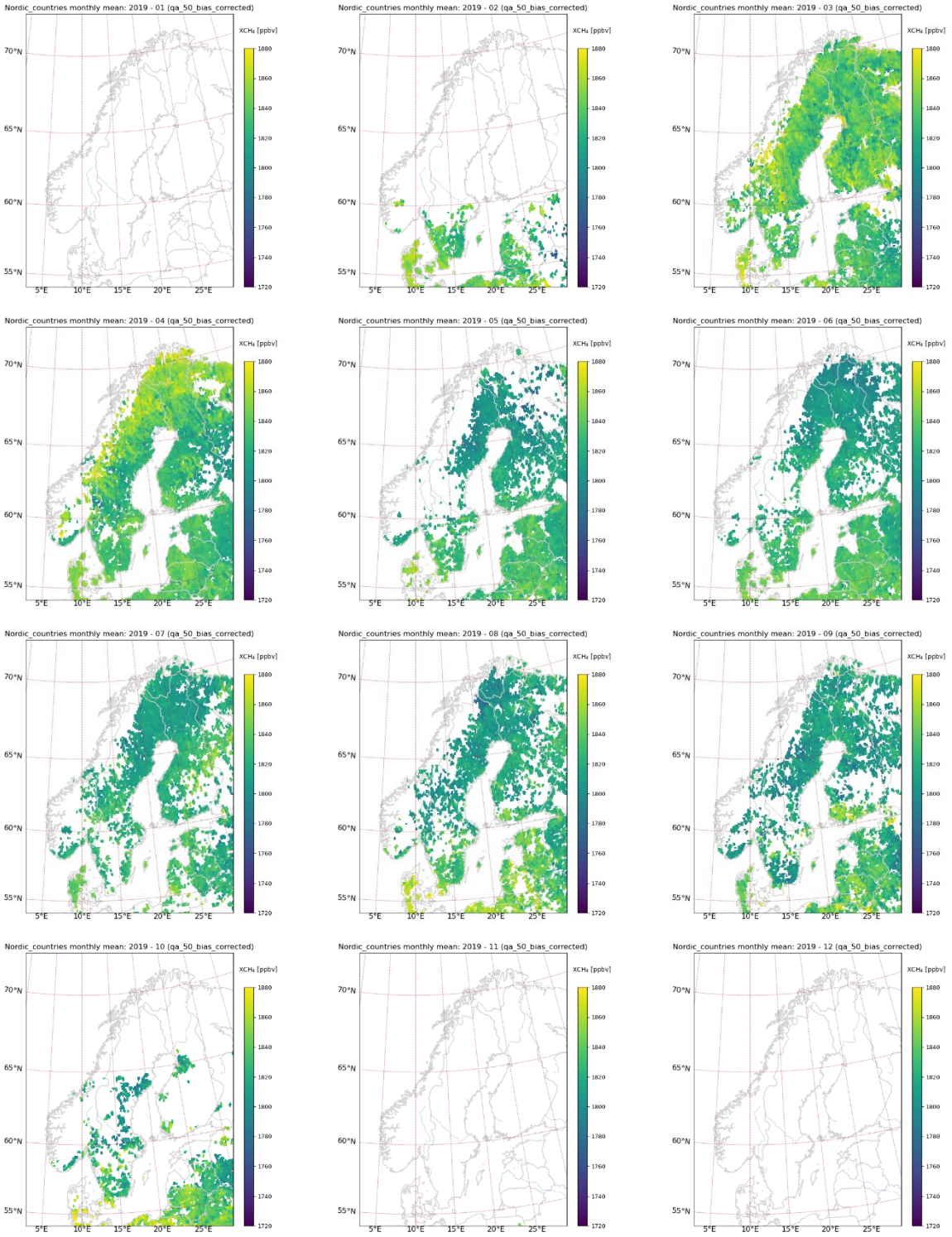


*Figure A2. Operational monthly mean bias corrected $XCH_4$ offline data with qa_value > 0.5 for the year 2019.*

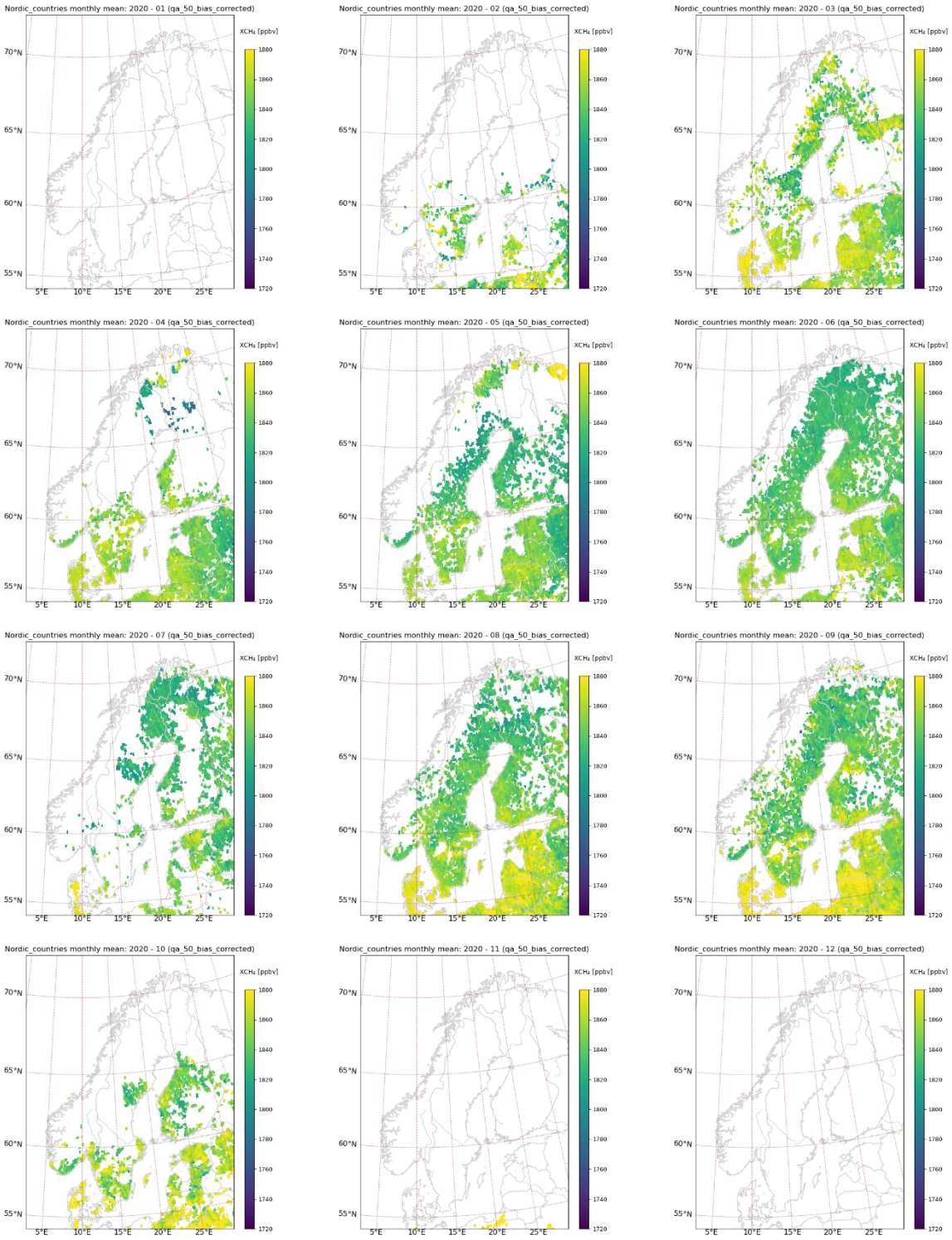


*Figure A3. Operational monthly mean bias corrected $XCH_4$ offline data with qa_value > 0.5 for the year 2020.*

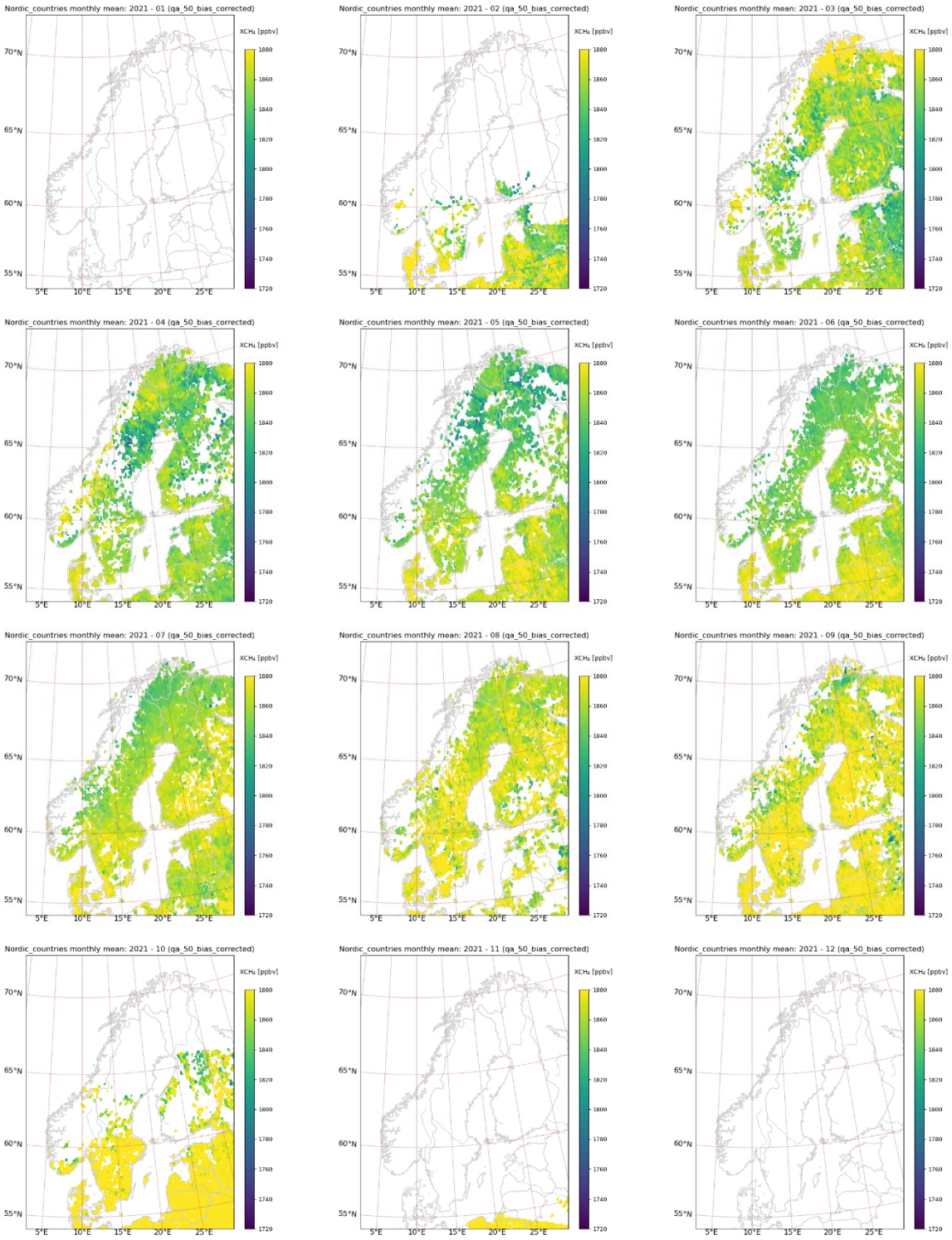


*Figure A4. Operational monthly mean bias corrected $XCH_4$ offline data with qa_value > 0.5 for the year 2021.*

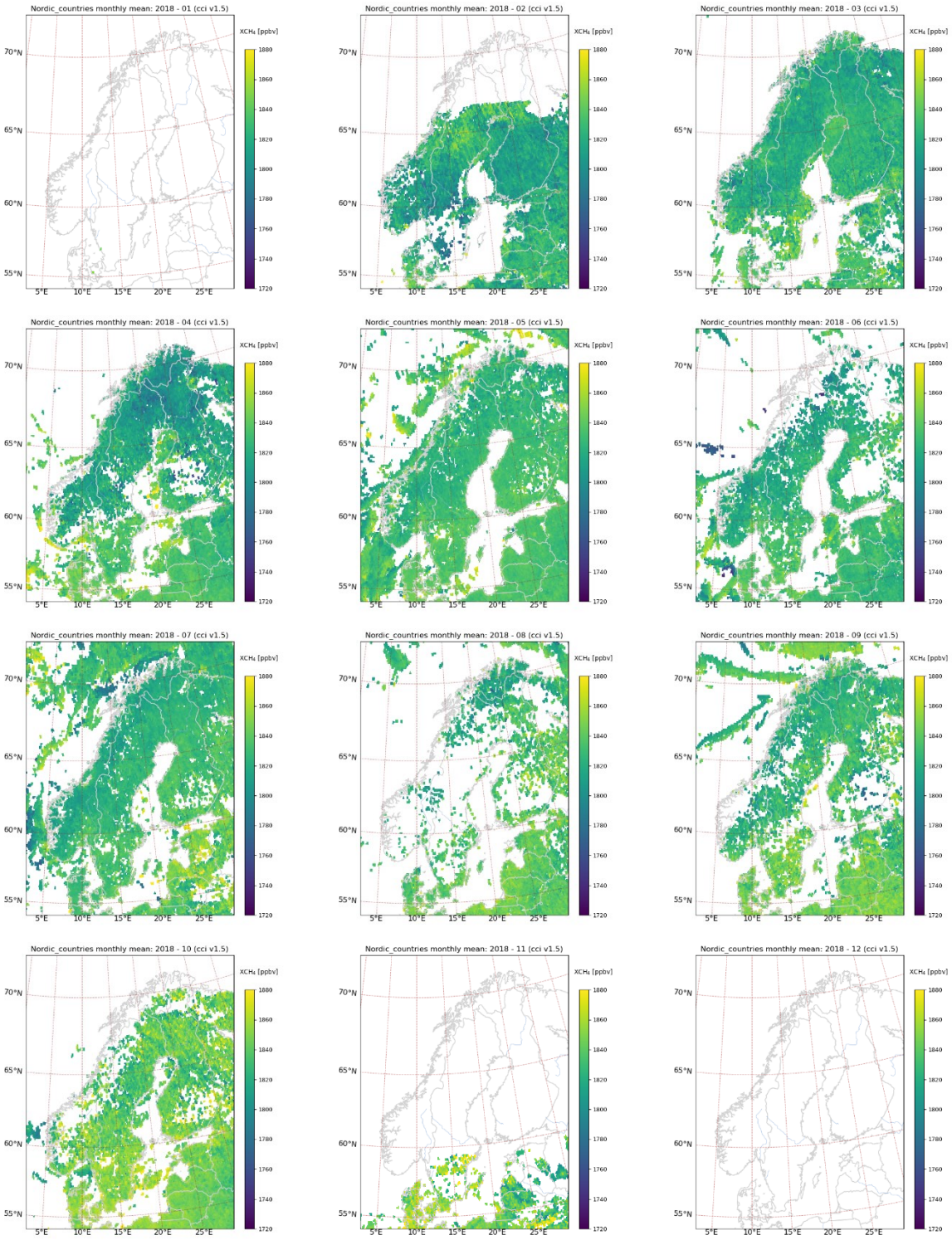


*Figure A5. Scientific monthly mean WFMD $XCH_4$ data version 1.5 for the year 2018.*

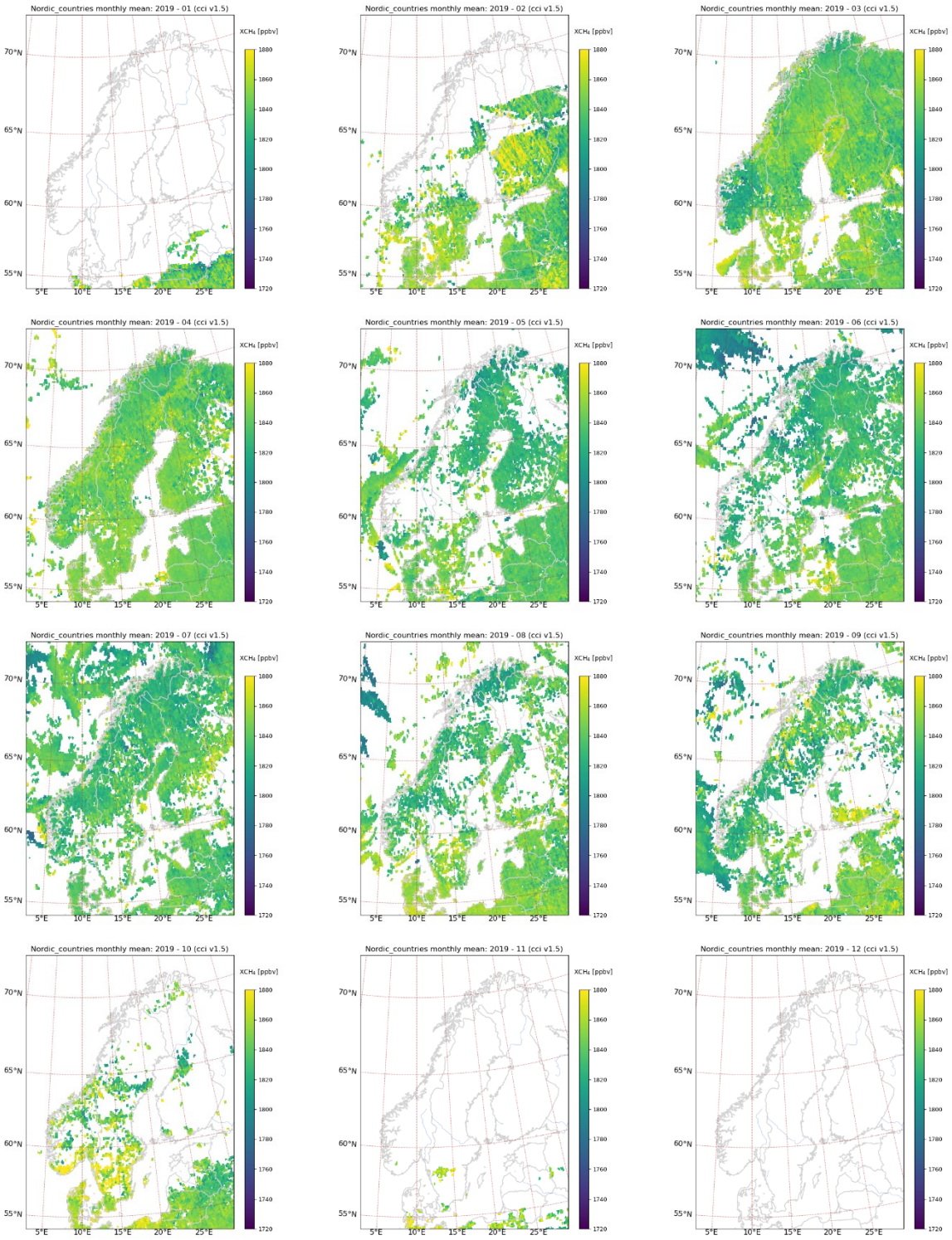


*Figure A6. Scientific monthly mean WFMD $XCH_4$ data version 1.5 for the year 2019.*

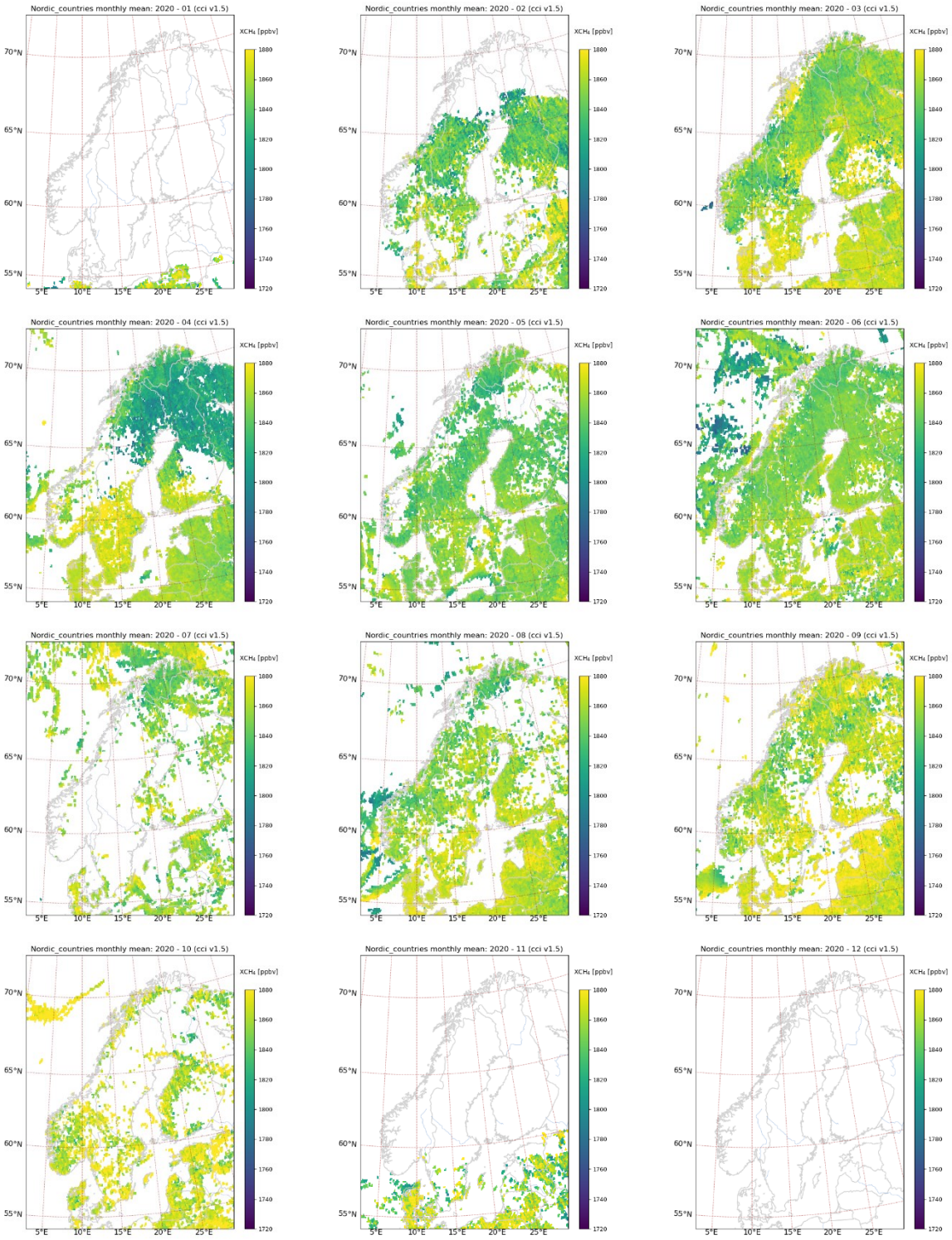


*Figure A7. Scientific monthly mean WFMD $XCH_4$ data version 1.5 for the year 2020.*

# Appendix B

# Monthly mean $XCH_4$ for the Northern latitudes (>50°N)

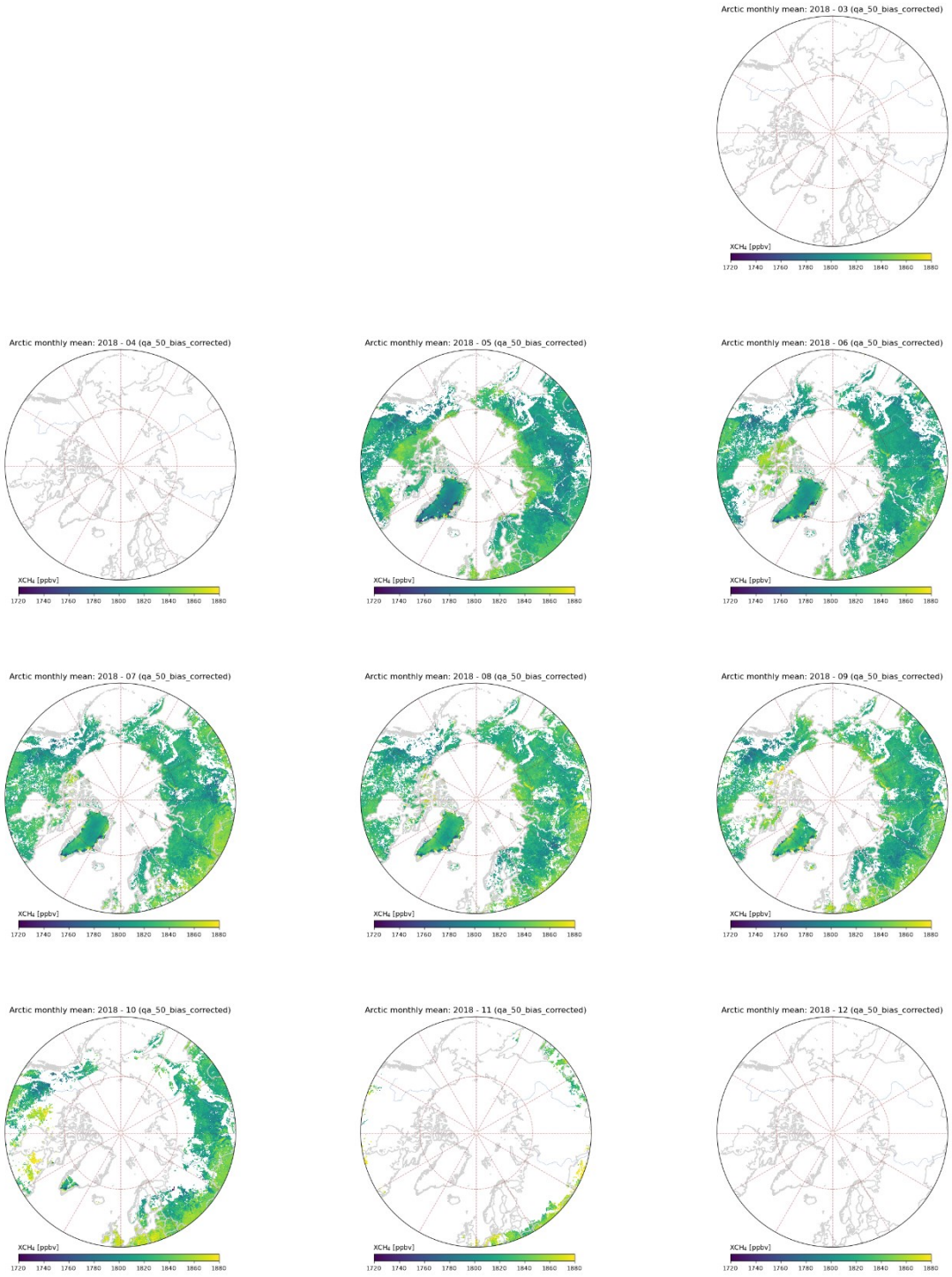


*Figure B1. Operational bias corrected $XCH_4$ for the year 2018 offline (OFFL – March, April, December) and reprocessed (RPRO – May - November) data with qa_value > 0.5.*

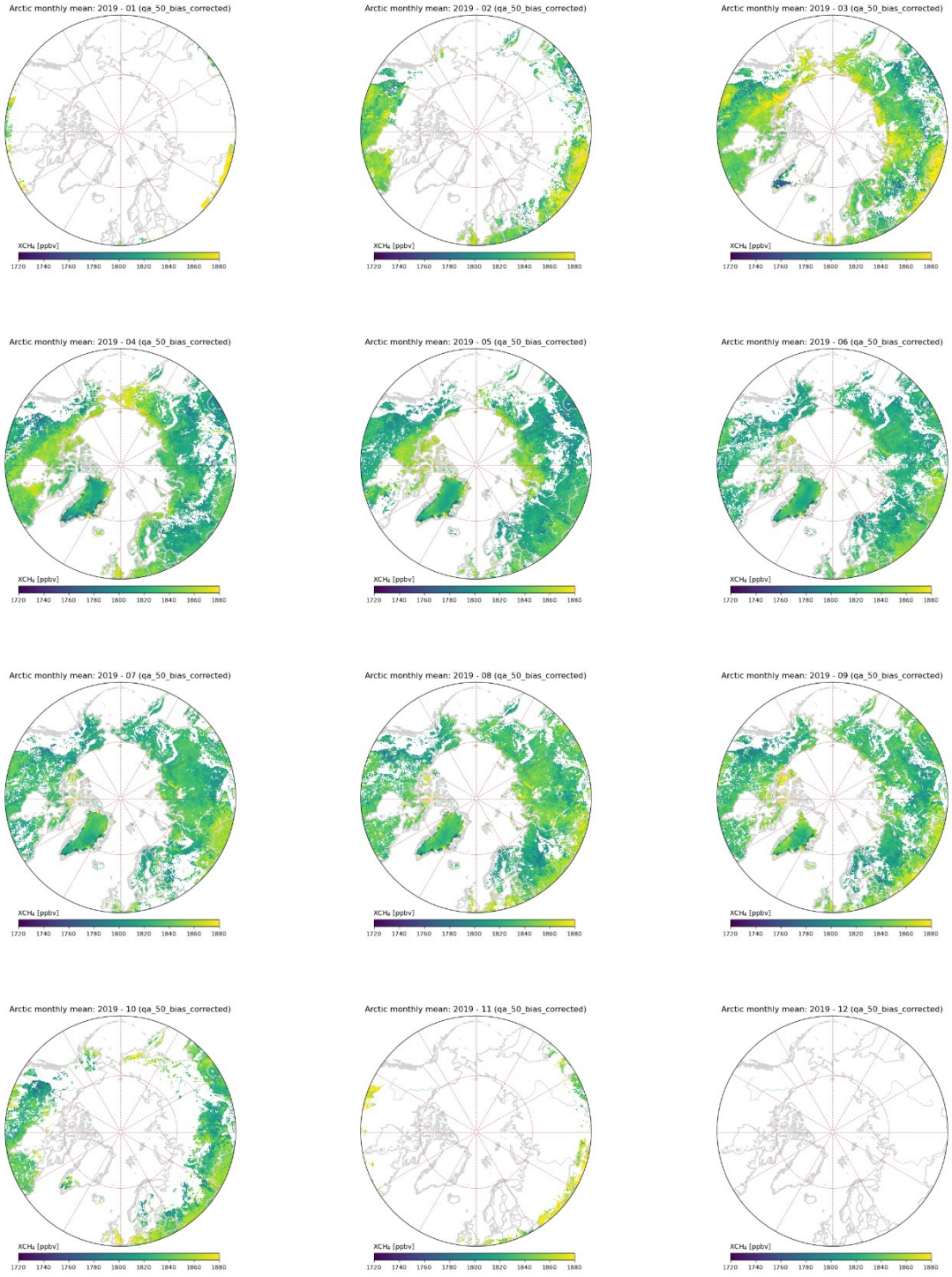


*Figure B2. Operational monthly mean bias corrected $XCH_4$ offline data with qa_value > 0.5 for the year 2019.*

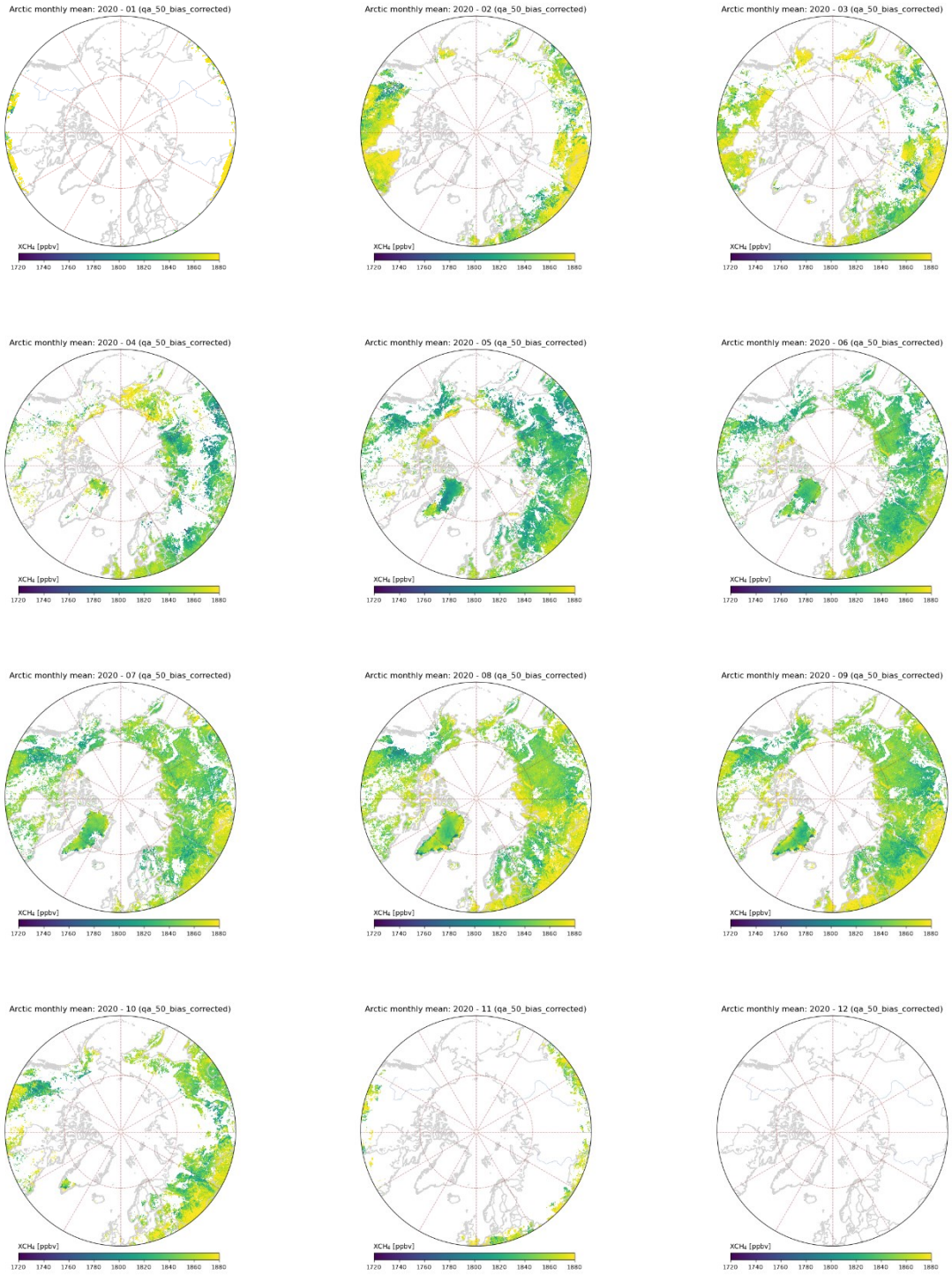


*Figure B3. Operational monthly mean bias corrected $XCH_4$ offline data with qa_value > 0.5 for the year 2020.*

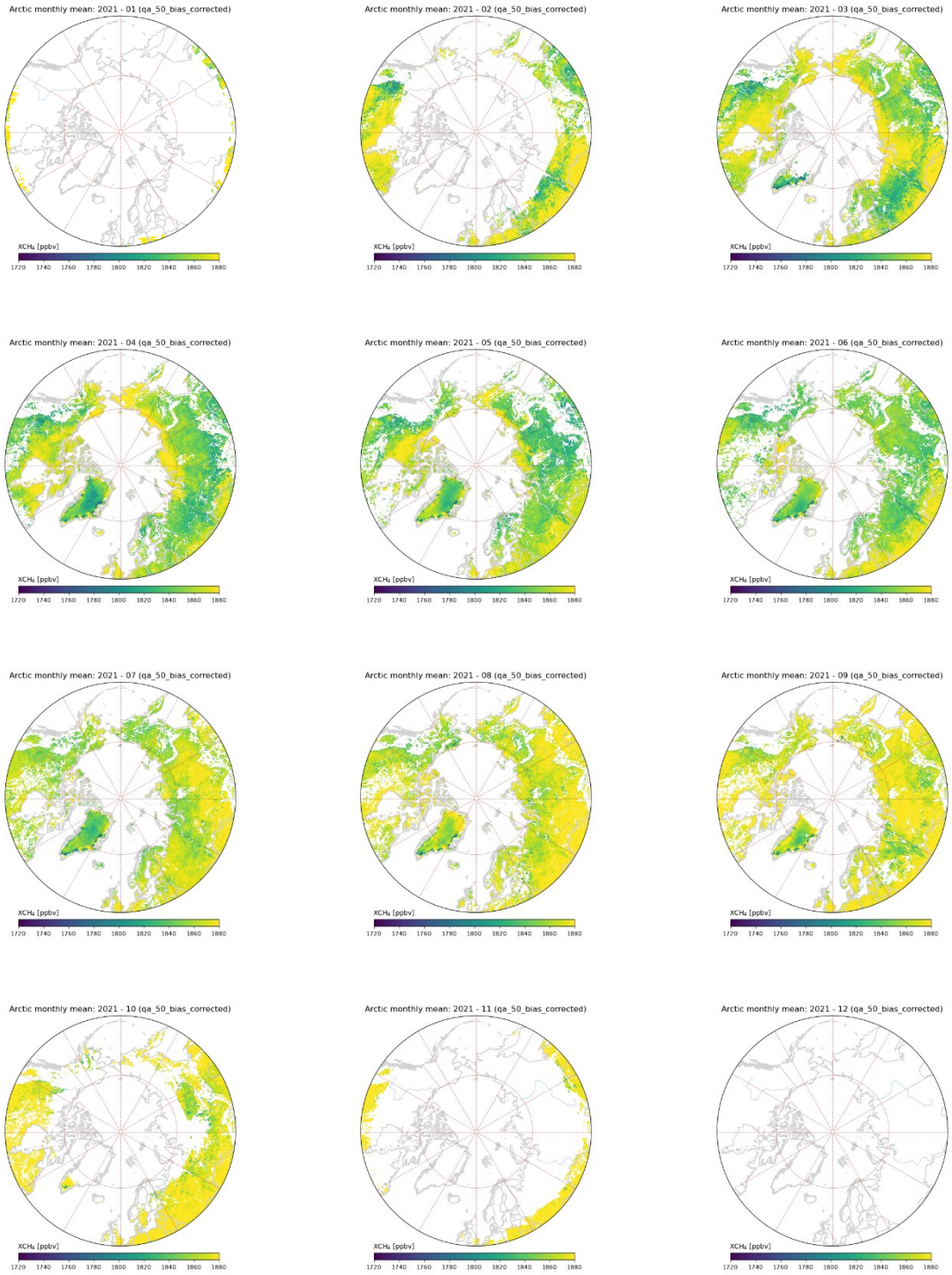


*Figure B4. Operational monthly mean bias corrected $XCH_4$ offline data with qa_value > 0.5 for the year 2021.*

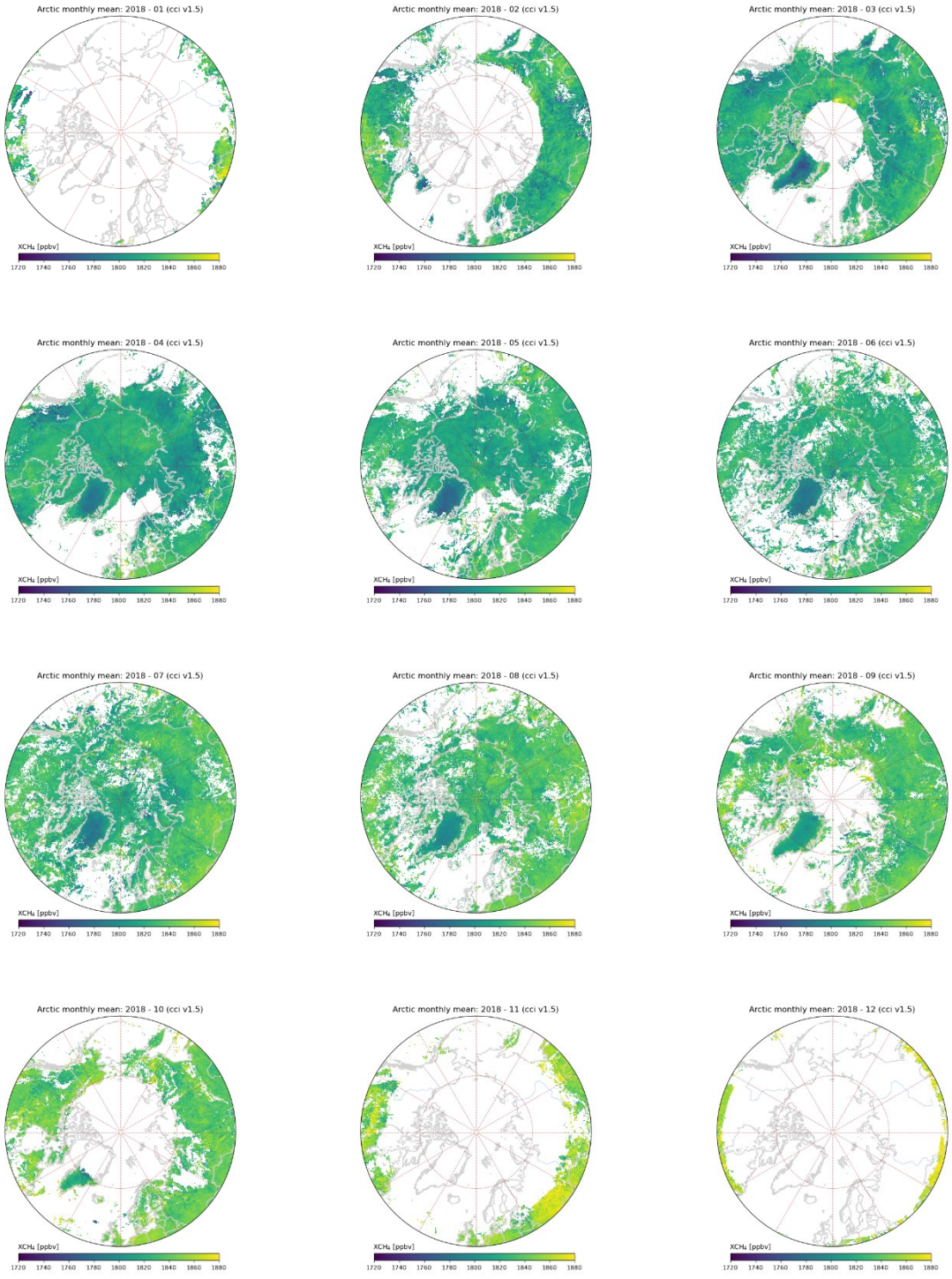


*Figure B5. Scientific monthly mean WFMD $XCH_4$ data version 1.5 for the year 2018.*

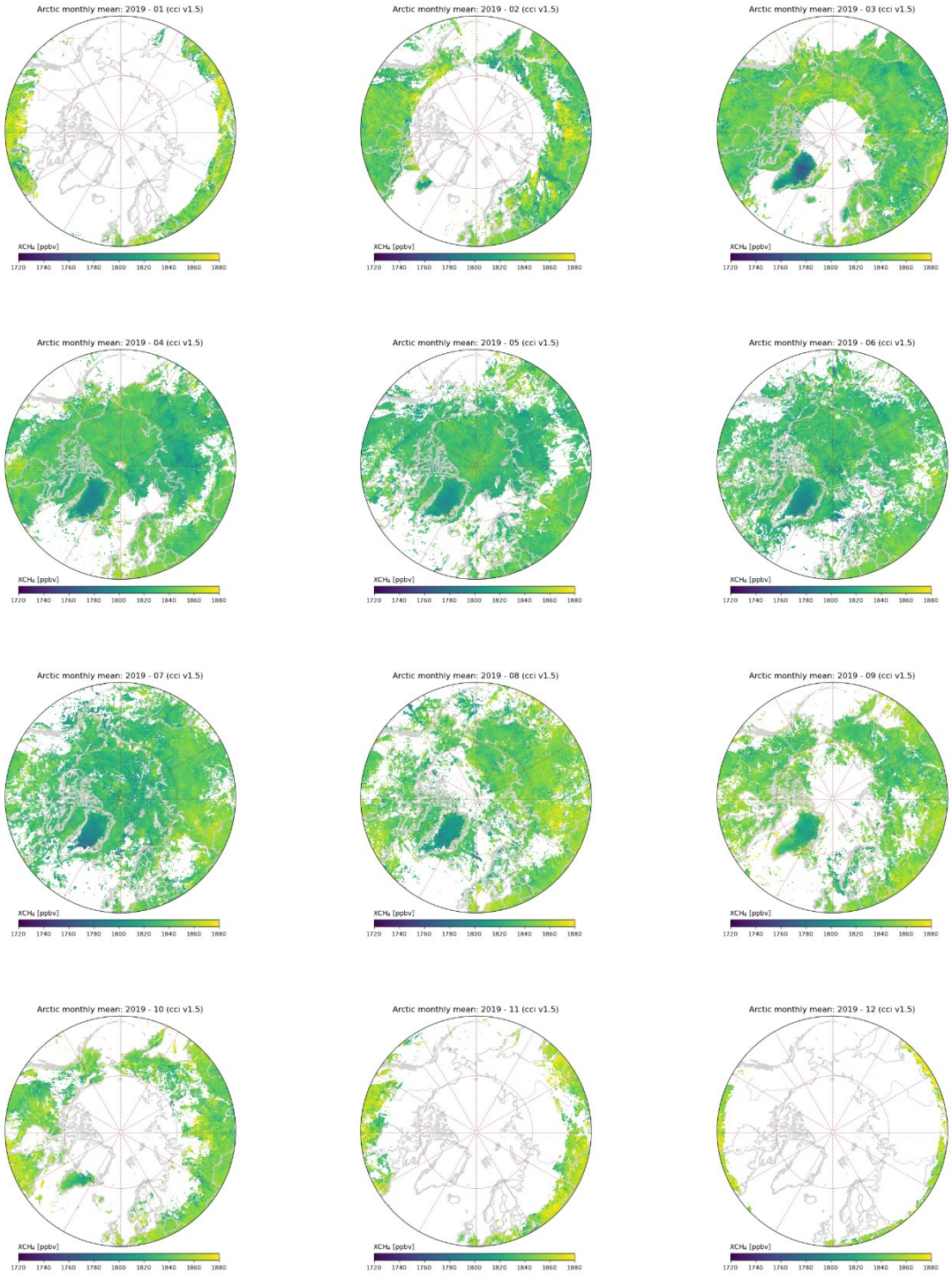


*Figure B6. Scientific monthly mean WFMD $XCH_4$ data version 1.5 for the year 2019.*

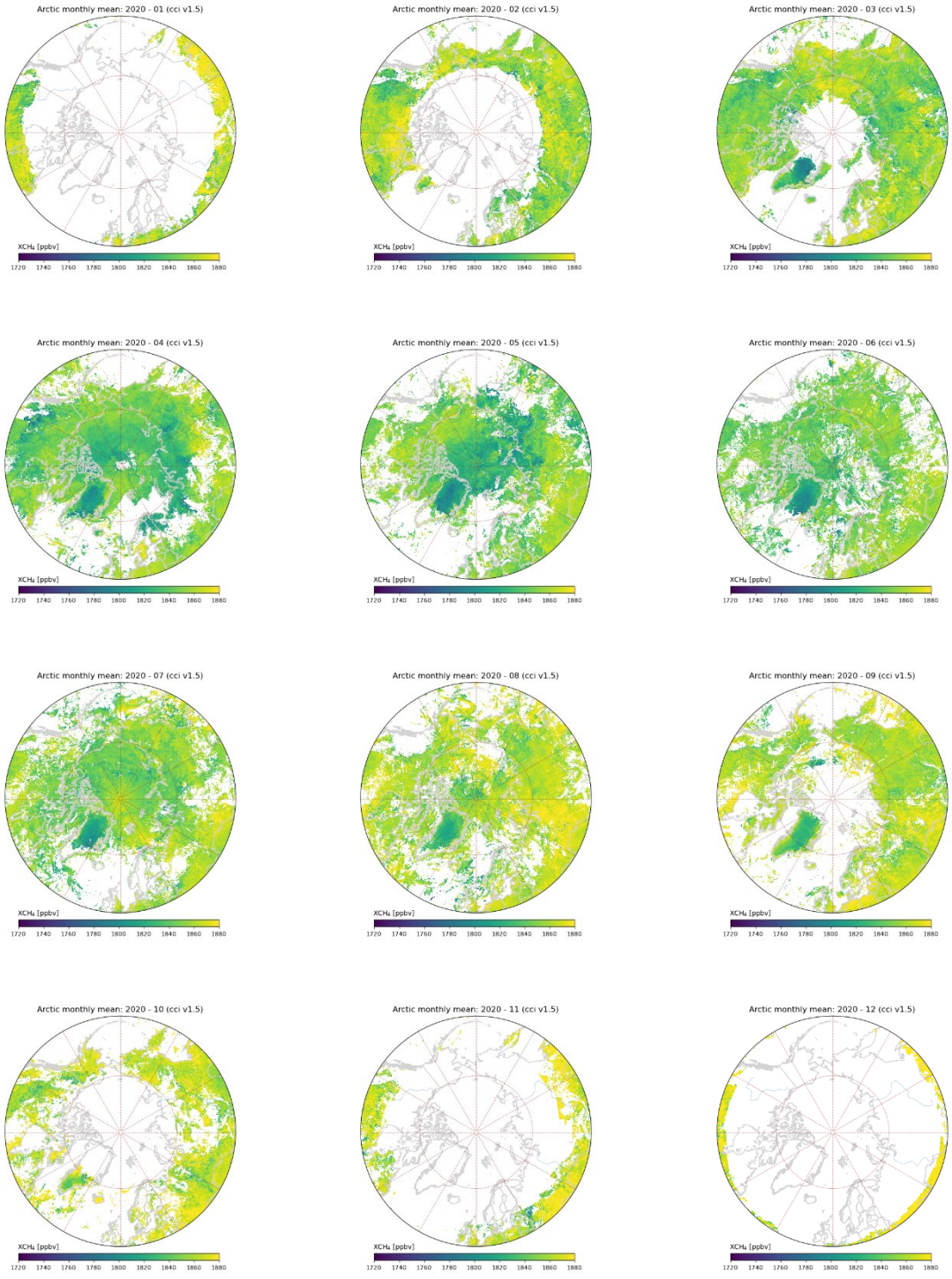


*Figure B7. Scientific monthly mean WFMD $XCH_4$ data version 1.5 for the year 2020.*

## NILU – Norwegian Institute for Air Research

NILU – Norwegian Institute for Air Research is an independent, non-profit institution established in 1969. Through its research NILU increases the understanding of climate change, of the composition of the atmosphere, of air quality and of hazardous substances. Based on its research, NILU markets integrated services and products within analysing, monitoring and consulting. NILU is concerned with increasing public awareness about climate change and environmental pollution.

*NILU's values:* *Integrity - Competence - Benefit to society*
*NILU's vision:* *Research for a clean atmosphere*

NILU – Norwegian Institute for Air Research
P.O. Box 100, NO-2027 KJELLER, Norway

E-mail: nilu@nilu.no
http://www.nilu.no

ISBN: 978-82-425-3084-4
ISSN: 2464-3327

Norsk institutt for luftforskning
Norwegian Institute for Air Research